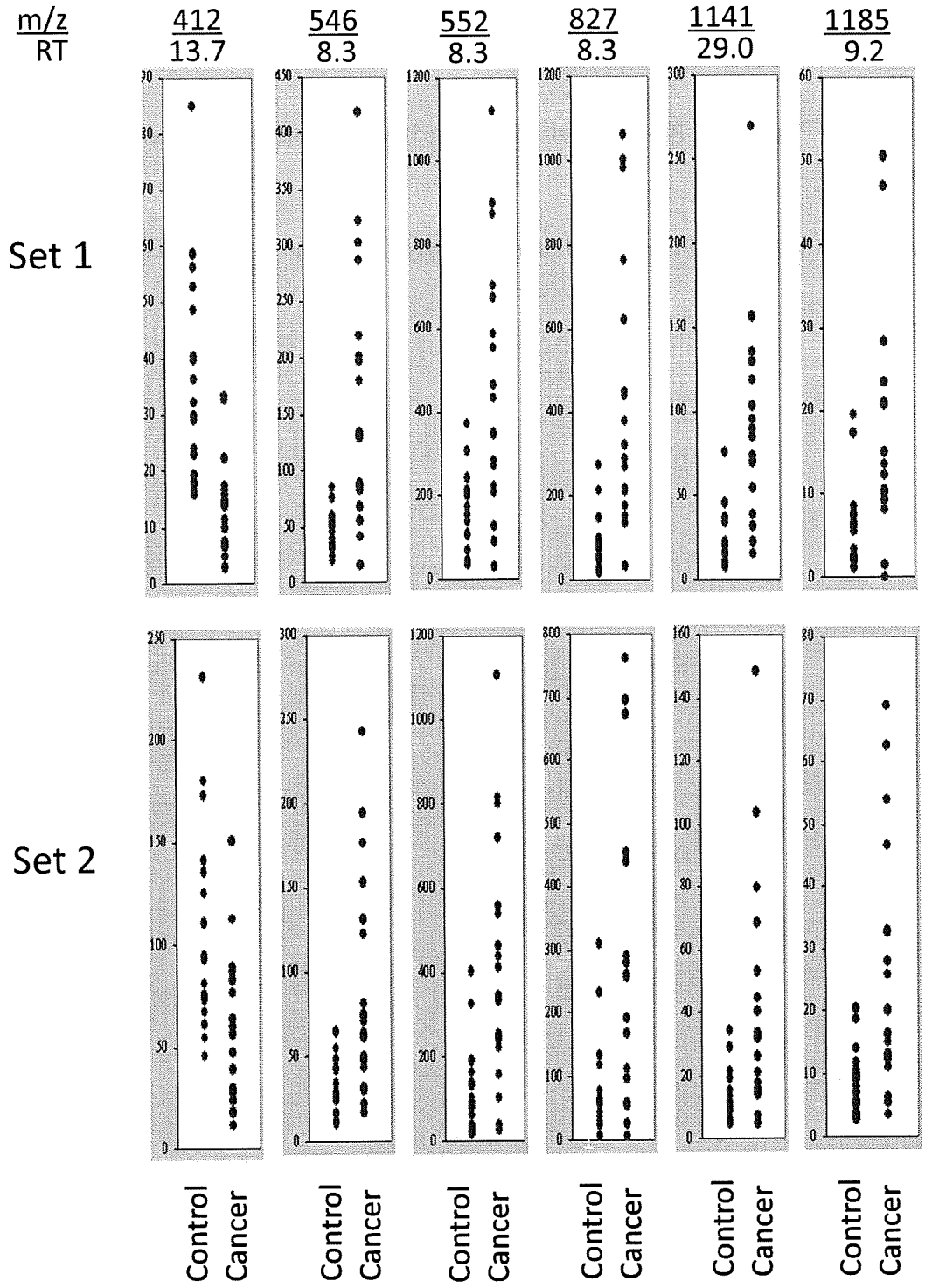

Supplementary Figure S1.
MS peaks whose intensity was significantly different between the pancreatic cancer patients and controls.
Distribution of intensity of the 6 MS peaks in Sets 1 and 2.

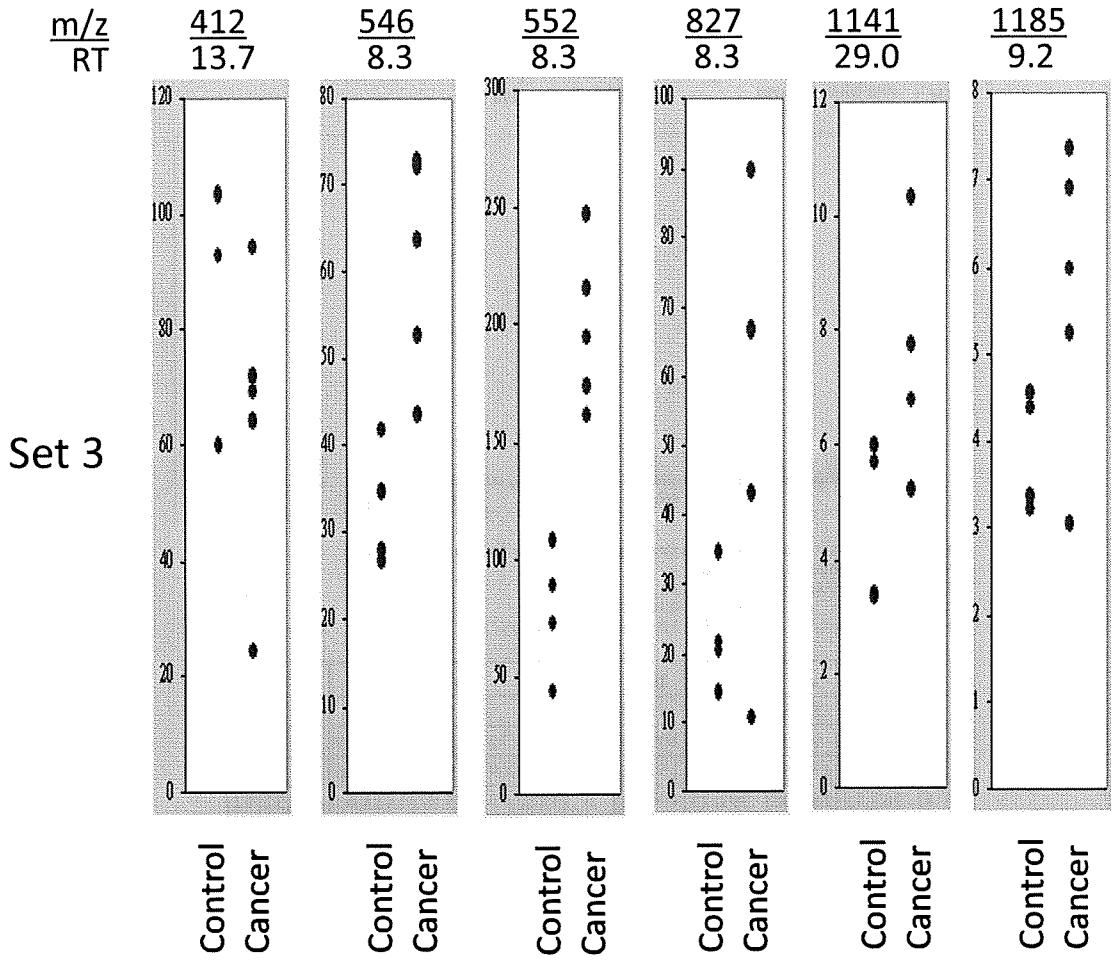

Supplementary Figure S2.
MS peaks whose intensity was significantly different between the pancreatic cancer patients and controls.
Distribution of intensity of the 6 MS peaks in Set 3.

Peptide View

MS/MS Fragmentation of ESSSHHPGIAEFPSR
Found in gi|182424, alpha-fibrinogen precursor

Match to Query 117: 1652.623754 from(827.319153,2+)
43977
From data file \\192.168.50.11\fs_project\2dical\Clinical Data\Pancreas
\search\082506C25-10-04-05-01\pkl\43977.txt

Or, Plot from 100 to 1500 Da

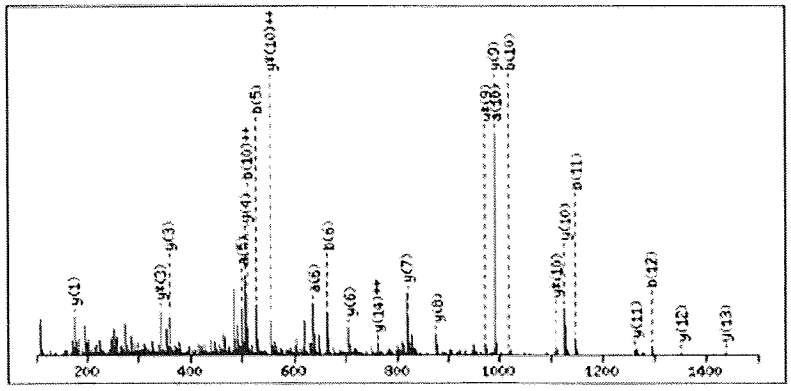

Monoisotopic mass of neutral peptide Mr(calc): 1652.75
Variable modifications:
P7 : Hydroxylation (P)
Ions Score: 65 **Expect:** 0.00039
Matches (Bold Red): 25/112 fragment ions using 58 most intense peaks

#	a	a^{++}	b	b^{++}	Seq.	y	y^{++}	y*	y^{*++}	#
1	102.05	51.53	130.05	65.53	E					15
2	189.09	95.05	217.08	109.04	S	1524.72	762.86	1507.69	754.35	14
3	276.12	138.56	304.11	152.56	S	1437.69	719.35	1420.66	710.83	13
4	363.15	182.08	391.15	196.08	S	1350.65	675.83	1333.63	667.32	12
5	500.21	250.61	528.20	264.61	H	1263.62	632.32	1246.60	623.80	11
6	637.27	319.14	665.26	333.14	H	1126.56	563.79	1109.54	555.27	10
7	750.32	375.66	778.31	389.66	P	989.51	495.26	972.48	486.74	9
8	807.34	404.17	835.33	418.17	G	876.46	438.73	859.43	430.22	8
9	920.42	460.71	948.42	474.71	I	819.44	410.22	802.41	401.71	7
10	991.46	496.23	1019.45	510.23	A	706.35	353.68	689.33	345.17	6
11	1120.50	560.75	1148.50	574.75	E	635.31	318.16	618.29	309.65	5
12	1267.57	634.29	1295.57	648.29	F	506.27	253.64	489.25	245.13	4
13	1364.62	682.82	1392.62	696.81	P	359.20	180.11	342.18	171.59	3
14	1451.65	726.33	1479.65	740.33	S	262.15	131.58	245.12	123.07	2
15					R	175.12	88.06	158.09	79.55	1

Supplementary Figure S3.
MS/MS spectrum of the peptide at 827 m/z and 8.3 min.

Peptide View

MS/MS Fragmentation of TFPGFFSPMLGEFVSETESR
Found in gi|182424, alpha-fibrinogen precursor

Match to Query 269: 2280.895116 from(1141.454834,2+)
83677
From data file \\192.168.50.11\fs_project\2dical\Clinical Data\Pancreas
\search\082506C25-10-04-05-01\pkl\83677.txt

Or, Plot from 100 to 1600 Da

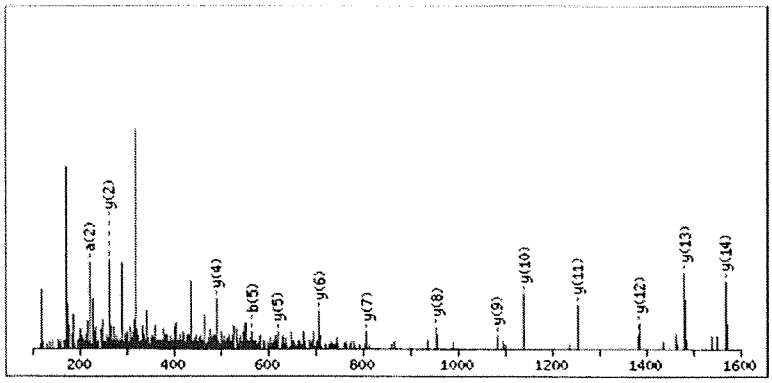

Monoisotopic mass of neutral peptide Mr(calc): 2280.04
Variable modifications:
P3 : Hydroxylation (P)
Ions Score: 65 **Expect:** 0.00039
Matches (Bold Red): 14/152 fragment ions using 39 most intense peaks

#	a	a^{++}	b	b^{++}	Seq.	y	y^{++}	y^*	y^{*++}	#
1	74.06	37.53	102.05	51.53	T					20
2	221.13	111.07	249.12	125.07	F	2180.00	1090.50	2162.97	1081.99	19
3	334.18	167.59	362.17	181.59	P	2032.93	1016.97	2015.91	1008.46	18
4	391.20	196.10	419.19	210.10	G	1919.88	960.45	1902.86	951.93	17
5	538.27	269.64	566.26	283.63	F	1862.86	931.94	1845.84	923.42	16
6	685.33	343.17	713.33	357.17	F	1715.79	858.40	1698.77	849.89	15
7	772.37	386.69	800.36	400.68	S	1568.73	784.87	1551.70	776.35	14
8	869.42	435.21	897.41	449.21	P	1481.69	741.35	1464.67	732.84	13
9	1000.46	500.73	1028.45	514.73	M	1384.64	692.82	1367.61	684.31	12
10	1113.54	557.28	1141.54	571.27	L	1253.60	627.30	1236.57	618.79	11
11	1170.57	585.79	1198.56	599.78	G	1140.52	570.76	1123.49	562.25	10
12	1299.61	650.31	1327.60	664.30	E	1083.50	542.25	1066.47	533.74	9
13	1446.68	723.84	1474.67	737.84	F	954.45	477.73	937.43	469.22	8
14	1545.74	773.38	1573.74	787.37	V	807.38	404.20	790.36	395.68	7
15	1632.78	816.89	1660.77	830.89	S	708.32	354.66	691.29	346.15	6
16	1761.82	881.41	1789.81	895.41	E	621.28	311.15	604.26	302.63	5
17	1862.87	931.94	1890.86	945.93	T	492.24	246.62	475.21	238.11	4
18	1991.91	996.46	2019.90	1010.46	E	391.19	196.10	374.17	187.59	3
19	2078.94	1039.97	2106.94	1053.97	S	262.15	131.58	245.12	123.07	2
20					R	175.12	88.06	158.09	79.55	1

Supplementary Figure S4.
MS/MS spectrum of the peptide at 1141 m/z and 29.0 min.

Supplementary Figure S5

A

```
  1 MFSMRIVCLV LSVVGTAWTA DSGEGDFLAE GGGVRGPRVV ERHQSACKDS
 51 DWPFCSDEDW NYKCPSGCRM KGLIDEVNQD FTNRINKLKN SLFEYQKNNK
101 DSHSLTTNIM EILRGDFSSA NNRDNTYNRV SEDLRSRIEV LKRKVIEKVQ
151 HIQLLQKNVR AQLVDMKRLE VDIDIKIRSC RGSWSRALAR EVDLKDYEDQ
201 QKQLEQVIAK DLLPSRDRQH LPLIKMKPVP DLVPGNFKSQ LQKVPPEWKA
251 LTDMPQMRME LERPGGNEIT RGGSTSYGTG SETESPRNPS SAGSWNSGSS
301 GPGSTGNRNP GSSGTGGTAT WKPGSSGPGS AGSWNSGSSG TGSTGNQNPG
351 SPRPGSTGTW NPGSSERGSA GHWTSESSVS GSTGQWHSES GSFRPDSPGS
401 GNARPNNPDW GTFEEVSGNV SPGTRREYHT EKLVTSKGDK ELRTGKEKVT
451 SGSTTTTRRS CSKTVTKTVI GPDGHKEVTK EVVTSEDGSD CPEAMDLGTL
501 SGIGTLDGFR HRHPDEAAFF DTASTGKTFP GFFSPMLGEF VSETESRGSE
551 SGIFTNTKES SSHHPGIAEF PSRGKSSSYS KQFTSSTSYN RGDSTFESKS
601 YKMADEAGSE ADHEGTHSTK RGHAKSRPVR GIHTSPLGKP SLSP
```

B

4-Hydroxyproline

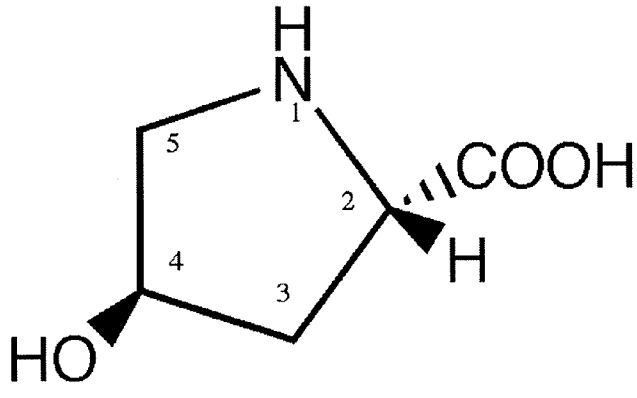

ESSSHHP(O)GIAEFPSR

TFP(O)GFFSPMLGEFVSETESR

Supplementary Figure S6

A

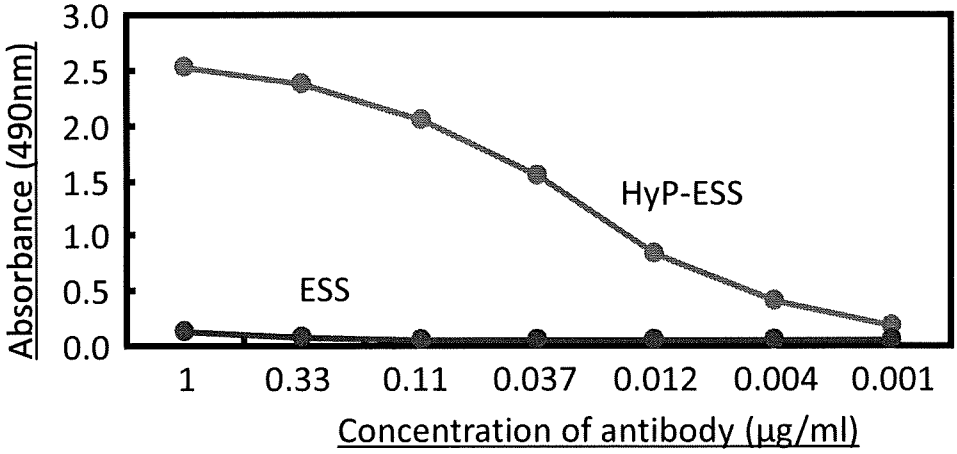

B

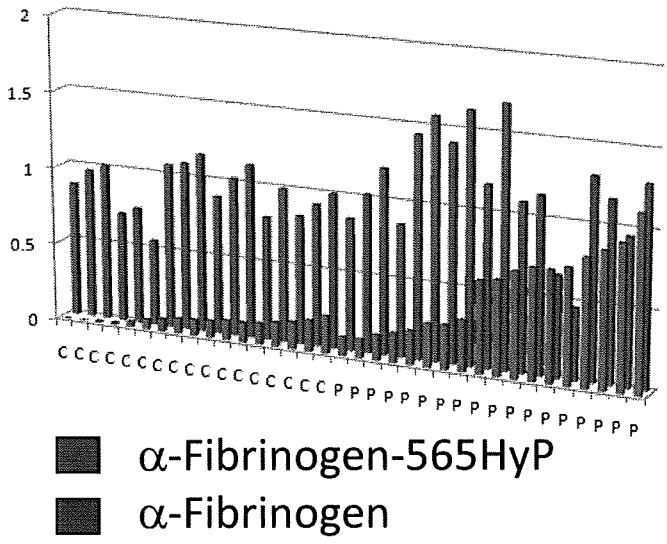

C

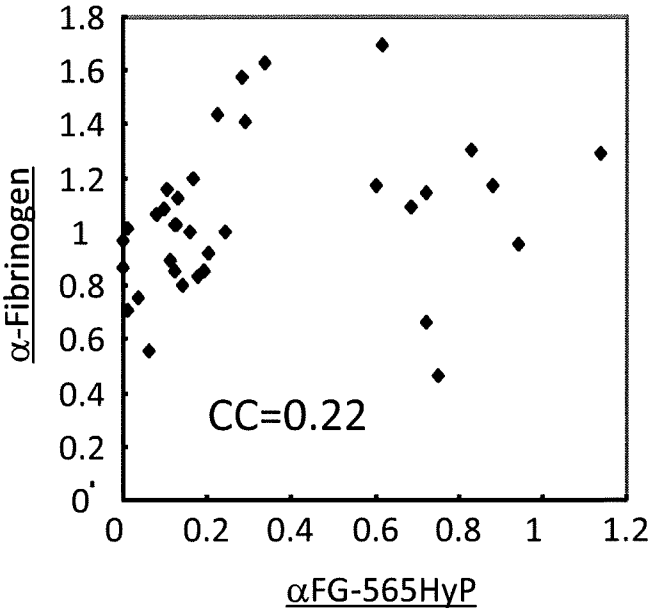

D

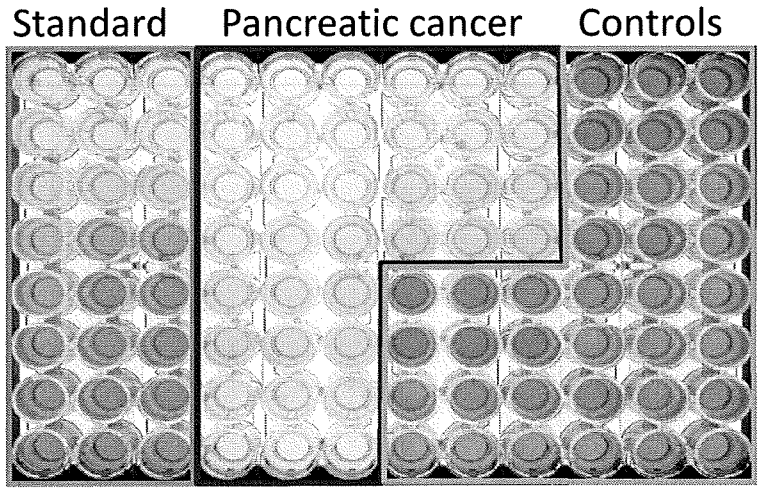

Supplementary Figure S7

A

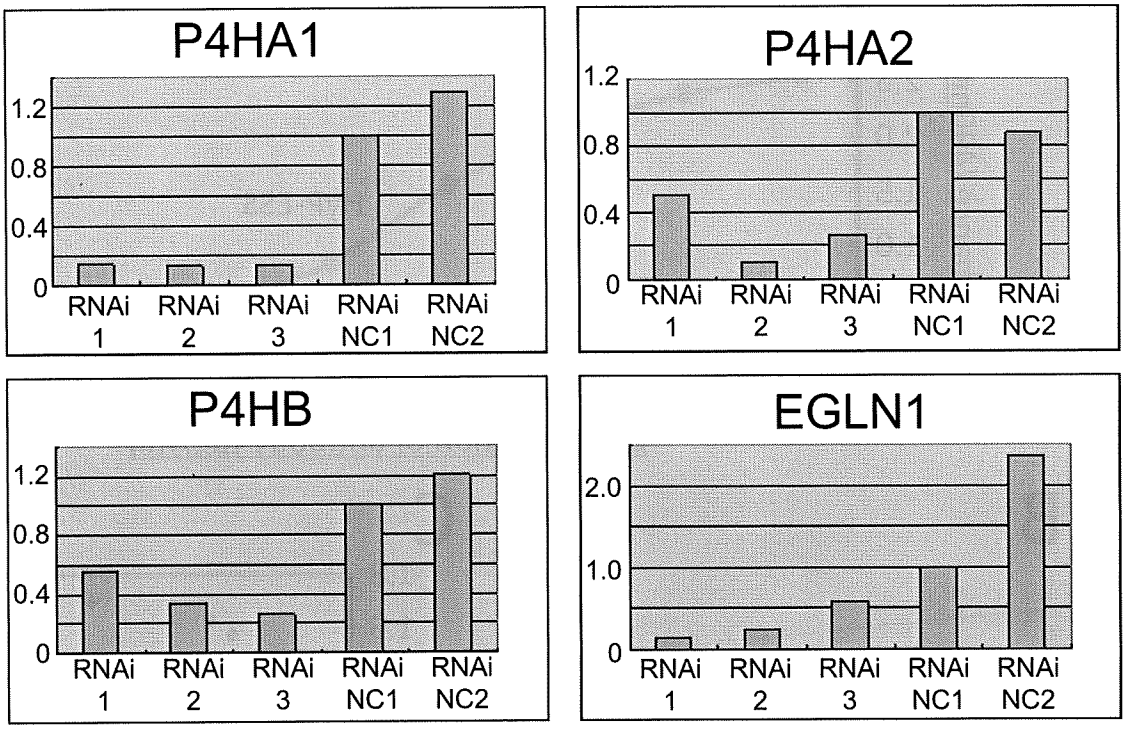

B

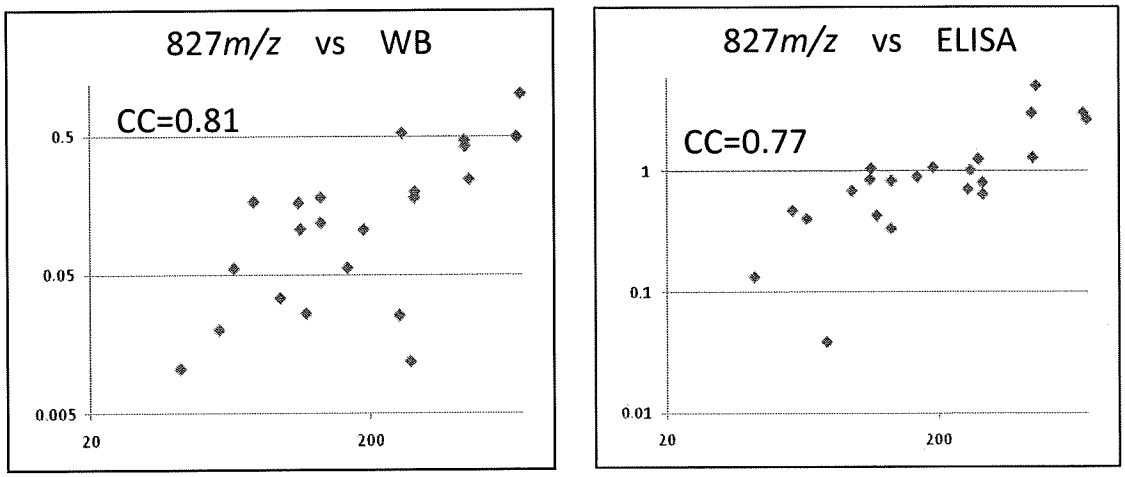

C

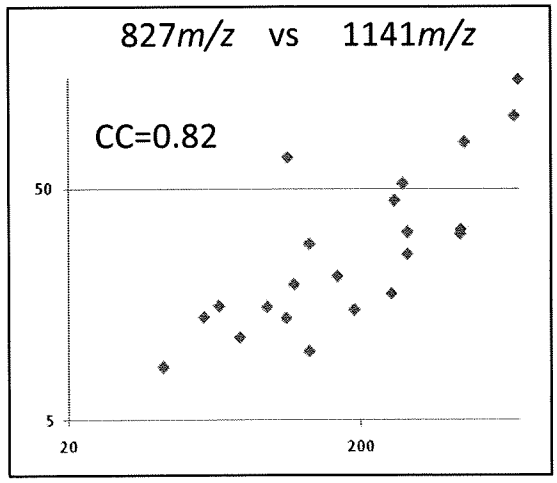

Supplementary Table S1

Intensity of peptide peaks that differed significantly between pancreatic cancer patients and healthy controls.

	Set 1 (18 cancer patients and 19 controls)			**Set 2** (20 cancer patients and 20 controls)		
Mass and RT	Control[1]	Cancer[1]	*P*-value[2]	Control[1]	Cancer[1]	*P*-value[2]
412 m/z, 13.7 min	35.3±18.2	14.1±8.6	7.02×10^{-6}	106.8±47.0	56.0±35.8	3.72×10^{-4}
546 m/z, 8.3 min	43.9±17.5	164.1±11.1	8.53×10^{-6}	32.4±17.5	88.2±62.3	7.94×10^{-5}
552 m/z, 8.3 min	147.4±92.6	457.3±304.8	2.35×10^{-4}	106.8±106.5	408.2±282.0	1.56×10^{-5}
827 m/z, 8.3 min	87.4±64.1	434.4±319.7	1.63×10^{-6}	73.7±81.5	282.9±228.4	4.19×10^{-4}
1141 m/z, 29.0 min	23.0±17.5	89.6±59.9	3.12×10^{-6}	17.3±12.2	52.6±49.7	3.27×10^{-4}
1185 m/z, 9.9 min	6.0±4.9	19.0±15.7	2.35×10^{-4}	8.3±4.9	25.1±19.1	1.04×10^{-4}

[1]Mean ± SD (in arbitrary unit determined by 2DICAL)

[2]Mann-Whitney *U* test (Control vs. Cancer)

Supplementary Table S2.

Plasma level of αFG-565HyP in pancreatic cancer patients with different stages.

		No. of cases	αFG-565HyP[1]	*P*-value[2]	CA19-9[3]	*P*-value[2]
Healthy control		113	0.91±1.24		11.5±11.1	
Pancreatic cancer	Total	160	2.26±2.28	3.80×10^{-15}	2117.9±3231.7	$<2.2\times10^{-16}$
	Stage IA[4]	2	1.10±1.45	0.8106	71.6±89.7	0.2106
	Stage IB[4]	4	3.43±3.81	0.02985	451.4±569.0	0.009444
	Stage IIA[4]	5	2.68±3.14	0.04045	174.5±190.4	0.001506
	Stage IIB[4]	28	2.15±2.39	3.067×10^{-5}	658.2±1079.6	2.404×10^{-13}
	Stage III[4]	41	1.93±1.71	3.392×10^{-7}	1963.0±3003.1	4.394×10^{-13}
	Stage IV[4]	78	2.42±2.43	1.878×10^{-12}	2897.2±3706.4	$<2.2\times10^{-16}$

[1]Mean ± SD (in arbitrary unit determined by competitive ELISA)

[2]Mann-Whitney *U* test (in comparison to "Healthy control")

[3]Mean ± SD (U/ml) measured with an immunoradiometric assay kit (Fujirebio Diagnostic, Malvern, PA)

[4]UICC stages (not available in 2 cases)

Supplementary Table S3.

Plasma level of αFG-565HyP in patients with different diseases.

	No. of cases	αFG-565HyP[1]	*P*-value[2]	CA19-9[3]	*P*-value[2]
Healthy control	113	0.91±1.24		11.5±11.1	
Pancreatic cancer	160	2.26±2.28	3.80×10^{-15}	2117.9±3231.7	$<2.2\times10^{-16}$
Chronic pancreatitis	12	1.30±0.74	0.03886	7.7±7.7	0.1504
Benign pancreatic tumor/cyst	37	1.12±1.31	0.2163	14.6±16.0	0.7751
Bile duct cancer	25	2.08±1.48	4.242×10^{-5}	961.8±2358.4	1.627×10^{-5}
Cholecystitis	22	0.51±0.53	0.1114	16.3±15.3	0.1939
Hepatocellular carcinoma	14	2.00±1.75	0.001077	61.6±167.9	0.1109
Esophageal cancer	10	1.96±0.77	0.0002065	17.7±14.2	0.07706
Gastric cancer	147	1.30±1.38	0.0005951	137.8±932.4	0.01655
Colorectal cancer	145	1.60±1.82	9.287×10^{-6}	75.2±357.7	0.00779

[1]Mean ± SD (in arbitrary unit determined by competitive ELISA)

[2]Mann-Whitney *U* test (in comparison to "Healthy control")

[3]Mean ± SD (U/ml)

MiR-21 is an EGFR-regulated anti-apoptotic factor in lung cancer in never-smokers

Masahiro Seike[a,b], Akiteru Goto[a], Tetsuya Okano[a,b], Elise D. Bowman[a], Aaron J. Schetter[a], Izumi Horikawa[a], Ewy A. Mathe[a], Jin Jen[c], Ping Yang[d], Haruhiko Sugimura[e], Akihiko Gemma[b], Shoji Kudoh[b], Carlo M. Croce[f,1], and Curtis C. Harris[a,1]

[a]Laboratory of Human Carcinogenesis, Center for Cancer Research, National Cancer Institute, National Institutes of Health, Bethesda, MD 20892; [b]Department of Pulmonary Medicine/Infection and Oncology, Nippon Medical School, Tokyo 113-8602, Japan; [c]Division of Pulmonary and Critical Care Medicine and Microarray Share Resources, Mayo Clinic and Foundation, Rochester, MN 55905; [d]Department of Health Sciences Research, Mayo Clinic College of Medicine, Rochester, MN 55905; [e]Department of Pathology, Hamamatsu University School of Medicine, Hamamatsu 431-3192, Japan; and [f]Molecular Virology, Immunology and Medical Genetics, Ohio State University Comprehensive Cancer Center, Columbus, OH 43212

Contributed by Carlo M. Croce, June 1, 2009 (sent for review January 12, 2009)

Fifteen percent of lung cancer cases occur in never-smokers and show characteristics that are molecularly and clinically distinct from those in smokers. Epidermal growth factor receptor (*EGFR*) gene mutations, which are correlated with sensitivity to EGFR-tyrosine kinase inhibitors (EGFR-TKIs), are more frequent in never-smoker lung cancers. In this study, microRNA (miRNA) expression profiling of 28 cases of never-smoker lung cancer identified aberrantly expressed miRNAs, which were much fewer than in lung cancers of smokers and included miRNAs previously identified (e.g., up-regulated miR-21) and unidentified (e.g., down-regulated miR-138) in those smoker cases. The changes in expression of some of these miRNAs, including miR-21, were more remarkable in cases with *EGFR* mutations than in those without these mutations. A significant correlation between phosphorylated-EGFR (*p*-EGFR) and miR-21 levels in lung carcinoma cell lines and the suppression of miR-21 by an EGFR-TKI, AG1478, suggest that the EGFR signaling is a pathway positively regulating miR-21 expression. In the never-smoker–derived lung adenocarcinoma cell line H3255 with mutant *EGFR* and high levels of *p*-EGFR and miR-21, antisense inhibition of miR-21 enhanced AG1478-induced apoptosis. In a never-smoker–derived adenocarcinoma cell line H441 with wild-type *EGFR*, the antisense miR-21 not only showed the additive effect with AG1478 but also induced apoptosis by itself. These results suggest that aberrantly increased expression of miR-21, which is enhanced further by the activated EGFR signaling pathway, plays a significant role in lung carcinogenesis in never-smokers, as well as in smokers, and is a potential therapeutic target in both *EGFR*-mutant and wild-type cases.

apoptosis | microRNA | microarray | EGFR-TKI | therapeutic target

Approximately 10% to 25% of all lung cancer cases are not attributable to smoking (1, 2). Recent studies that pay specific attention to lung cancers in never-smokers have suggested that these cancers have characteristics distinct from those in smokers (2): G-to-T transversions of the *p53* and *K-ras* mutations occur less frequently in lung adenocarcinomas from never-smokers than in those from smokers (3–6), and mutations of epidermal growth factor receptor (*EGFR*) gene are observed more frequently in never-smoker cases (6). A profiling of global gene expression in never-smoker lung cancers may provide novel molecular and clinical aspects in lung carcinogenesis. Although EGFR tyrosine kinase inhibitors (EGFR-TKIs), including gefitinib and erlotinib, currently are in clinical use and are preferentially effective in *EGFR*-mutant cases (7, 8), as many as 30% of *EGFR*-mutant cases and 90% of *EGFR* wild-type cases showed no therapeutic response to EGFR-TKIs (9). Therefore, identification of a new therapeutic target and development of a method to improve the EGFR-TKI therapy will be of critical importance for the better treatment of lung cancer.

MicroRNAs (miRNAs) are small, non-coding RNA molecules of about 18 to 25 nucleotides that frequently are located at chromosomal regions deleted or amplified in cancers, suggesting that miRNAs are a class of genes involved in human tumorigenesis (10). Expression levels of miRNAs are altered in various types of human cancers, including lung cancers (11–18). Recently, miRNAs have been demonstrated to be diagnostic and prognostic markers in leukemia, lung cancer, and colon cancer (13, 18–19). It also is suggested that miRNAs can be a therapeutic target in human cancers (20). We previously analyzed miRNA expression profiles of 104 lung cancers, 99 of which were from smokers, and found that high expression of miR-155, miR-21, and miR-106a, as well as low expression of let-7a, correlated with poor survival (18). In the present study we investigate a global expression profile of miRNAs in lung cancers from never-smokers. Comparisons of miRNA expression in never-smoker versus smoker cases and in *EGFR* wild-type versus mutant cases find different profiles of miRNA expression associated with smoking status and reveal EGFR-mediated regulation of miRNA expression. Our in vitro functional analyses also suggest that the inhibition of miR-21, whose up-regulation is associated with *EGFR* mutations, can be a potential therapeutic strategy in combination with EGFR-TKI treatment or by itself.

Results

MicroRNA Expression Profiles in Lung Cancers from Never-Smokers. We examined miRNA expression profiles in 28 matched pairs of lung cancer and noncancerous lung tissues from never-smokers (Table 1 and supporting information (SI) Table S1) using the Ohio State miRNA microarray version 3.0 (21). In class comparison analysis using National Cancer Institute Division of Treatment and Diagnosis Biometric Research Branch (BRB) array tools, 18 miRNAs were found to be differentially expressed in cancers compared with noncancerous tissues [$P < 0.01$ with a false-discovery rate (FDR) of < 0.15)] (Table 2). The expression profiles of these 18 miRNAs distinguished cancer and paired noncancerous tissues with a prediction accuracy of 84% using the 3-nearest-neighbor algorithm and an accuracy of 82% using the support vector machine algorithm within BRB array tools (10-fold cross validation repeated 100 times). Expression levels of 5 miRNAs were higher in cancer tissues, with miR-21 enriched the most, at 2.35-fold. Expression levels of 13 miRNAs were lower in cancers, with miR-486 and miR-126* repressed the most, at 0.45-fold. The validity of the analysis was supported by the identification of a single miRNA by

Author contributions: M.S., A. Goto, I.H., E.A.M., A. Gemma, C.M.C., and C.C.H. designed research; M.S., A. Goto, T.O., E.D.B., A.J.S., I.H., and C.C.H. performed research; E.D.B., J.J., P.Y., H.S., S.K., and C.M.C. contributed new reagents/analytic tools; M.S., A. Goto, A.J.S., I.H., E.A.M., C.M.C., and C.C.H. analyzed data; and M.S., I.H., C.M.C., and C.C.H. wrote the paper.

The authors declare no conflict of interest.

Data deposition: The microRNA microarray data have been deposited in the Gene Expression Omnibus (GEO) (http://www.ncbi.nlm.nih.gov/geo/, GSE14936).

[1]To whom correspondence may be addressed. E-mail: Curtis_Harris@nih.gov or carlo.croce@osumc.edu.

This article contains supporting information online at www.pnas.org/cgi/content/full/0905234106/DCSupplemental.

Table 1. Characteristics of never-smoker patients with non-small cell lung cancer

Characteristic	No. of patients
Histology	
Adenocarcinoma	22 (78%)
Squamous cell carcinoma	4 (14%)
Adenosquamous cell carcinoma	1 (4%)
Unclassified	1 (4%)
Stage	
I	21 (75%)
II–IV	7 (25%)
Age	
≤ 65	18 (64%)
> 65	10 (36%)
Gender	
Female	18 (64%)
Male	10 (36%)
Race	
Caucasian	19 (68%)
African American	3 (11%)
Asian (Japanese)	6 (21%)
EGFR gene status	
Wild-type	22 (79%)
Mutant	6 (21%)

2 different probes (miR-21, miR-521, and miR-516a), of 2 mature miRNAs generated from a single stem-loop pre-miRNA (miR-126 and miR-126*), and of more than 1 miRNA chromosomally clustered and possibly co-regulated (miR-30a and miR-30c on 6q13; miR-30b and miR-30d on 8q24.22; and miR-516a, miR-520, and miR-521 on 19q13.41)]. The mRNA microarray data of never-smoker lung adenocarcinoma cases (22) (http://www.ncbi.nlm.nih.gov/geo/, accession number = GSE10072) also showed that 2 host genes, *TMEM49* and *EGFL7* (Table 2), were differentially expressed in cancer and noncancerous tissues in the same directions as their resident miRNAs (miR-21 and miR-126/126*, respectively). The expression levels of 3 miRNAs (miR-21, miR-126, and miR-486) were examined by real-time quantitative RT-PCR (qRT-PCR) (Fig. S1). MiR-21 expression was significantly higher in cancer tissues than in noncancerous tissues ($P < 0.05$, paired t-test) (Fig. S1*A*), and miR-126 and miR-486 were expressed at significantly lower levels in cancers (each $P < 0.05$, paired t-test) (Fig. S1 *B* and C), further validating the results of the microarray analysis.

Differential miRNA Profiles in Lung Cancers from Never-Smokers Versus Smokers. To identify cancer-associated changes in miRNA expression that are related to smoking status, we compared the miRNA expression profiles of the present never-smoker cases with those of 58 smoker lung adenocarcinoma cases in our previous study (18) and 23 additional cases of lung adenocarcinoma in smokers (Table S2). We identified 5 miRNAs that commonly were changed in expression in never-smoker and smoker cases, among which was the increased miR-21 (Table S3). Although only 2 miRNAs, miR-138 and let-7c, were changed significantly (both were down-regulated) in never-smoker cases, the altered expression of 36 miRNAs was preferentially associated with smoker cases (Table S3), probably reflecting the more extensive genetic and epigenetic changes in smoker-derived lung cancers (23). By qRT-PCR we validated the specific down-regulation of miR-138 in never-smoker adenocarcinomas and the up-regulation of miR-21 and the down-regulation of miR-126* irrespective of smoking status (Fig. S2). Interestingly, miR-138 is located at chromosome 3p21.33, a candidate locus that carries a lung cancer suppressor gene (24), and was reported to target the human telomerase reverse transcriptase gene (*hTERT*) (25) on which a variety of cellular and viral oncogenic mechanisms act (26). A role for this miRNA in the etiology of lung cancers from never-smokers deserves further investigation.

MiRNA Expression Profiles Associated with *EGFR* Gene Mutations. The status of the *EGFR* gene was determined by DNA sequencing in the

Table 2. miRNAs differentially expressed in lung cancer tissues and normal lung tissues from 28 never-smokers

Mature miR	Probe	Location	P-value†	FDR‡	Type§	Ratio¶	Host gene‖
miR-21	hsa-mir-21-prec-17	17q23.1	3.0E-04	0.01	Up	2.35	*TMEM49*
miR-21	hsa-mir-21–1	17q23.1	9.6E-04	0.03	Up	2.22	*TMEM49*
miR-141	hsa-mir-141-prec-1	12p13.31	0.001	0.03	Up	1.50	Intergenic
miR-210	hsa-mir-210-prec	11p15.5	0.002	0.06	Up	1.51	Intergenic
miR-200b	hsa-mir-200b	1p36.33	0.008	0.11	Up	1.39	Intergenic
miR-346	hsa-mir-346	10q23.2	0.009	0.12	Up	1.14	*GRID-1*
miR-126*	hsa-mir-126*-1	9q34.3	3.5E-05	0.01	Down	0.45	*EGFL7*
miR-126	hsa-mir-126	9q34.3	0.004	0.07	Down	0.69	*EGFL7*
miR-30a	hsa-mir-30a-prec-1	6q13	1.4E-04	0.01	Down	0.61	*C6orf155*
miR-30d	hsa-mir-30d-prec-2	8q24.22	1.5E-04	0.01	Down	0.57	Intergenic
miR-486	hsa-mir-486	8p11.21	2.7E-04	0.01	Down	0.45	Intergenic
miR-129	hsa-mir-129–2	11p11.2	2.8E-04	0.01	Down	0.77	Intergenic
miR-451	hsa-mir-451–1	17q11.2	4.8E-04	0.02	Down	0.46	Intergenic
miR-521	hsa-mir-521–2	19q13.41	0.005	0.08	Down	0.84	Intergenic
miR-521	hsa-mir-521–1	19q13.41	0.005	0.08	Down	0.80	Intergenic
miR-138	hsa-mir-138–1-prec	3p21.33	0.006	0.10	Down	0.72	Intergenic
miR-30b	hsa-mir-30b-prec	8q24.22	0.006	0.10	Down	0.58	Intergenic
miR-30c	hsa-mir-30c-prec	6q13	0.007	0.11	Down	0.61	*C6orf155*
miR-516a	hsa-mir-516a-1	19q13.41	0.008	0.11	Down	0.89	Intergenic
miR-516a	hsa-mir-516a-2	19q13.41	0.010	0.12	Down	0.90	Intergenic
miR-520	hsa-mir-520 h	19q13.41	0.009	0.12	Down	0.84	Intergenic

†miRNA-microarray analysis was performed using pairs of tumors and corresponding normal tissues from 28 never-smokers ($P < 0.01$).
‡False-discovery rate (FDR) < 0.15.
§Up, up-regulated in tumors compared with normal tissue; down, down-regulated in tumors compared with normal tissue.
¶Ratio of tumor to normal tissue.
‖http://microrna.sanger.ac.uk/sequences/.

Table 3. miRNAs differentially expressed in *EGF*-mutant and wild-type lung cancers from never-smokers

Mature miR	Probe	Location	P-value†	FDR†	Type§	Ratio¶
miR-21	hsa-mir-21–1	17q23.1	0.001	0.05	Up	1.79
	hsa-mir-21-prec-17	17q23.1	0.001	0.04	Up	1.67
miR-210	hsa-mir-210-prec	11p15.5	0.007	0.13	Up	1.20
miR-129	hsa-mir-129–2	11p11.2	0.001	0.05	Up	1.06
miR-486	hsa-mir-486	8p11.21	0.001	0.04	Down	0.60
miR-126	hsa-mir-126–2	9q34.3	0.003	0.08	Down	0.69
miR-126*	hsa-mir-126*-1	9q34.3	0.0005	0.04	Down	0.70
miR-138	hsa-mir-138–1-prec	3p21.33	0.004	0.10	Down	0.69
miR-521	hsa-mir-521–1	19q13.41	0.005	0.11	Down	0.81
	hsa-mir-521–2	19q13.41	0.003	0.08	Down	0.82
miR-451	hsa-mir-451–1	17q11.2	0.002	0.07	Down	0.81
miR-141	hsa-mir-141-prec-1	12p13.31	0.004	0.10	Down	0.85
miR-30d	hsa-mir-30d-prec-2	8q24.22	0.001	0.04	Down	0.93
miR-30a	hsa-mir-30a-prec-1	6q13	0.001	0.04	Down	0.95

†Class comparison analysis was performed between 22 *EGFR* wild-type and 6 mutant tumors ($P < 0.01$).
‡False-discovery rate (FDR) < 0.15.
§Up, up-regulated in *EGFR*-mutant compared with wild-type tumors; down, down-regulated in *EGFR*-mutant compared with wild-type tumors.
¶Ratio of tumors with mutant *EGFR* to tumors with wild-type *EGFR*.

28 lung cancer tissues from never-smokers, and 6 cases were found to have the activating mutations of *EGFR* in the tyrosine kinase domain (Table S1). The class comparison analysis of miRNA expression between 22 *EGFR* wild-type and 6 *EGFR*-mutant cases found 12 miRNAs that were significantly more or less abundant in *EGFR*-mutant cases ($P < 0.01$ with FDR < 0.15) (Table 3). Of the 12 miRNAs, 10 (miR-21, miR-210, miR-486, miR-126, miR-126*, miR-138, miR-521, miR-451, miR-30d, and miR-30a) were changed in the same direction as in cancer versus noncancerous tissues (Table 2), suggesting that *EGFR* mutations may reinforce the aberrant regulation of some miRNAs associated with lung carcinogenesis in never-smokers. MiR-21 and miR-486, which were most up-regulated and most down-regulated, respectively, in cancerous versus noncancerous tissues, again showed the greatest difference between *EGFR*-mutant and wild-type cancers (≈1.7-fold and 0.60-fold, respectively). Although the qRT-PCR data shown in Fig. S1 reflect a limited number of cases, limiting our ability to show a statistically significant difference between *EGFR*-mutant and wild-type cases in the expression of miR-21, miR-126, or miR-486, the 3 cases expressing the highest levels of miR-21 in cancer (cases 24, 25, and 28) had the activating mutation of *EGFR* (Fig. S1*A* and Table S1).

Expression of miR-21 and the Status of EGFR Signaling in Lung Cancer Cell Lines. Because of its most remarkable increase in cancer as compared with noncancerous tissues and its association with *EGFR* mutations, an indicator of sensitivity to EGFR-TKIs (9), miR-21 was chosen for further analyses. To investigate a correlation between miR-21 expression levels and the status of EGFR signaling pathway, 8 non-small cell lung cancer (NSCLC) cell lines were examined in Western blot (Fig. S3 *A*, *B*, and *C*) and qRT-PCR analyses (Fig. 1*A*). Among them, 3 adenocarcinoma cell lines (H3255, H1975, and H1650) were mutant for *EGFR*, as reported (8, 27–29). These 3 *EGFR*-mutant cell lines had high levels of phosphorylated EGFR (*p*-EGFR), as well as increased amounts of total EGFR protein and induction of phosphorylated Akt (*p*-Akt) (Fig. S3*C*), consistent with the constitutive activation of the EGFR signaling pathway in these cells (28, 29). Of the 3 cell lines, H3255 and H1975, but not H1650, expressed elevated levels of miR-21 (Fig. 1*A*). Of 5 *EGFR* wild-type cell lines, 3, either with (H441) or without (A549 and H1299) detectable levels of *p*-EGFR (Fig. S3 *A* and *B*), also expressed significantly higher levels of miR-21 than seen in control untransformed cells (Fig. 1*A*). The quantitative comparison of miR-21 and *p*-EGFR levels showed a significant positive correlation between these 2 factors (Pearson's correlation,

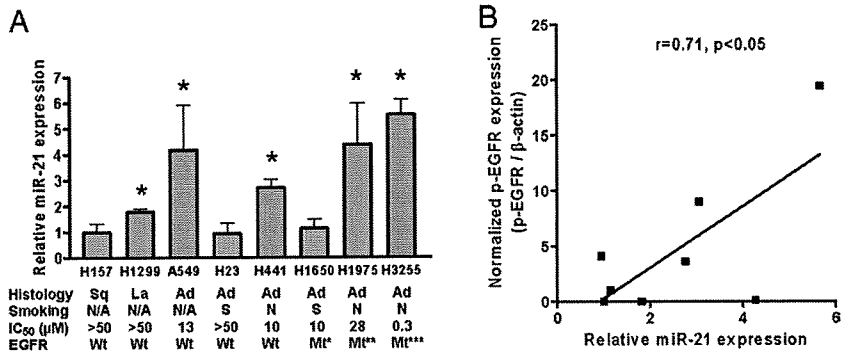

Fig. 1. MiR-21 expression in human lung cancer cell lines. (*A*) MiR-21 expression levels were analyzed by qRT-PCR and expressed relative to *hTERT*-immortalized normal human bronchial epithelial cells (HBET2) (defined as 1.0, not shown). Data were mean ± SD from 3 independent experiments. The suppressive effects of AG1478 on cell growth were determined by MTS assay and indicated as IC_{50}. *, $P < 0.05$ when compared with HBET2, Student's *t*-test. Ad, adenocarcinoma; La, large cell carcinoma; Mt*, *EGFR* mutant ΔE746-A750 (in-frame deletion of codons 746 to 750); Mt**, L858R (substitution from leucine to arginine at codon 858) and T790M (substitution from threonine to methionine at codon 790); Mt***, L858R; N/A, information not available; N, derived from never-smoker cases; S, derived from smoker cases; Sq, squamous cell carcinoma; Wt, *EGFR* wild-type. (*B*) Correlation between miR-21 expression and *p*-EGFR levels (Pearson's correlation, $r = 0.71$, $P < 0.05$). The miR-21 data were from panel *A*, and the *p*-EGFR data were obtained by quantitatively analyzing the results shown in Fig. S3.

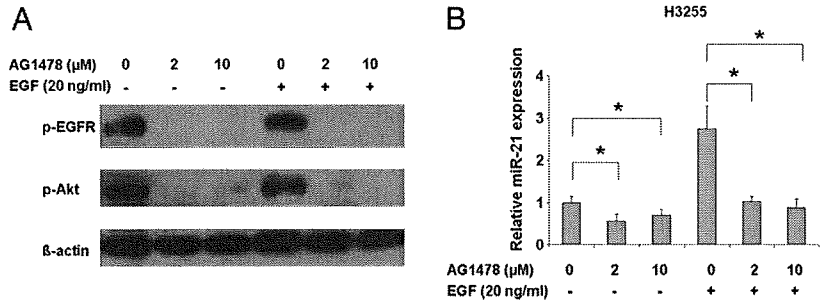

Fig. 2. AG1478 represses miR-21 expression. H3255 lung adenocarcinoma cells, characterized by a high expression of miR-21 and *EGFR* mutation, were serum starved for 24 h and then were grown in either the presence or absence of AG1478 (2 μM or 10 μM) for 2 h with or without following exposure to 20 ng/mL EGF for 15 min. (*A*) The effect of AG1478 on *p*-EGFR and *p*-Akt expression. β-actin was a loading control. (*B*) MiR-21 expression levels analyzed by qRT-PCR after the AG1478 treatments (2 μM or 10 μM) with or without EGF ligand stimulation. MiR-21 expression levels were expressed as values relative to untreated cells in the absence of EGF. Data were mean ± SD from 4 independent experiments. *, $P < 0.05$, paired *t*-test.

$r = 0.71, P < 0.05$) (Fig. 1*B*). These results suggest that the activated EGFR signaling pathway can be functionally associated with miR-21 up-regulation. It also was noteworthy that miR-21 expression and/or *EGFR* status correlated with sensitivity (indicated as IC_{50}) to an EGFR-TKI, AG1478 (Fig. 1*A*); the 5 cell lines showing AG1478-inhibited cell proliferation either had mutant *EGFR* (H1650) or expressed > 2-fold increased levels of miR-21 (H441 and A549), or both (H3255 and H1975). We selected 2 lung adenocarcinoma cell lines derived from never-smoker cancers for the functional assays of miR-21: H3255 with high sensitivity to AG1478 (IC_{50}, 0.3 μM), mimicking never-smoker lung cancer cases with mutant *EGFR* and the highest levels of miR-21 (e.g., case numbers 24, 25, and 28 in Fig. S1*A* and Table S1); and H441 with intermediate sensitivity to AG1478 (IC_{50}, 10 μM), mimicking never-smoker lung cancer cases with wild-type *EGFR* but with significantly increased levels of miR-21 (e.g., case numbers 5 and 23 in Fig. S1*A* and Table S1).

Activated EGFR Signaling Enhances miR-21 Expression. *EGFR*-mutant H3255 cells were treated with AG1478 in the presence or absence of EGF (Fig. 2). AG1478 at either 2 μM or 10 μM effectively inhibited the EGFR signaling under conditions with or without EGF ligand stimulation, as shown by diminished *p*-EGFR and *p*-Akt (Fig. 2*A*), consistent with the IC_{50} value of 0.3 μM in this cell line. The levels of miR-21 expression in the absence of EGF were significantly repressed by treatment with either concentration of AG1478 ($P < 0.01$, paired *t*-test) (Fig. 2*B*, *Left*). The addition of EGF resulted in ≈2.5-fold up-regulation of miR-21 expression, which still was inhibited back to the basal levels by treatment with either concentration of AG1478 ($P < 0.05$, paired *t*-test) (Fig. 2*B*, *Right*). These results indicate that miR-21 expression is positively regulated by the activated EGFR signaling in cancer cells with an activating *EGFR* mutation and that EGFR-TKIs can effectively repress the aberrantly increased miR-21. In H441 cells with wild-type *EGFR*, AG1478 at 10 μM (equivalent to the IC_{50} value in this cell line), but not at 2 μM, significantly repressed miR-21 expression ($P < 0.05$, paired *t*-test) (Fig. S4). Thus, the activated signaling from wild-type EGFR in H441 cells (Fig. S3*B*), probably through a self-produced TGF-alpha stimulation (28), also can be inhibited by AG1478, resulting in the repression of miR-21.

Antisense Inhibition of miR-21 Induces Apoptosis in Cooperation with EGFR-TKI. H3255 and H441 cells were transfected with an antisense oligonucleotide targeting miR-21 (anti-miR-21). The antisense-mediated repression of miR-21 in these cells was confirmed by qRT-PCR (Fig. 3*A*). Because miR-21 reportedly has an anti-apoptotic activity (30), we used an assay measuring caspase-3 and caspase-7 enzymatic activities to determine whether inhibition of miR-21 induces apoptosis in these cells (Fig. 3 *B* and *C*). In H3255 cells, anti-miR-21 alone did not induce apoptosis (Fig. 3*B*, *Left*). Notably, however, when used in combination with AG1478 at 0.2 μM (a concentration slightly lower than the IC_{50} value), anti-miR-21 significantly enhanced AG1478-induced apoptotic response (Fig. 3*B*, *Right*). In H441 cells, anti-miR-21 by itself resulted in a significant increase in apoptotic response (Fig. 3*C*, *Left*), although it was less effective than AG1478 treatment at 10 μM (a concentration equivalent to the IC_{50} value). Similar to the combinational effect observed in H3255 cells, anti-miR-21 further enhanced apoptotic response induced by 10 μM of AG1478 in H441 cells (Fig. 3*C*, *Right*). The effect of anti-miR-21 on apoptosis was substantiated further by Western blot analysis of poly (ADP-ribose) polymerase (PARP), a main cleavage target of caspase-3 in the apoptotic response (Fig. 3*D*). The amounts of uncleaved PARP were markedly decreased in H3255 cells treated with both anti-miR-21 and AG1478 and in H441 cells treated with anti-miR-21 in the presence or absence of AG1478, where anti-miR-21 caused significant increases in caspase 3/7 activities.

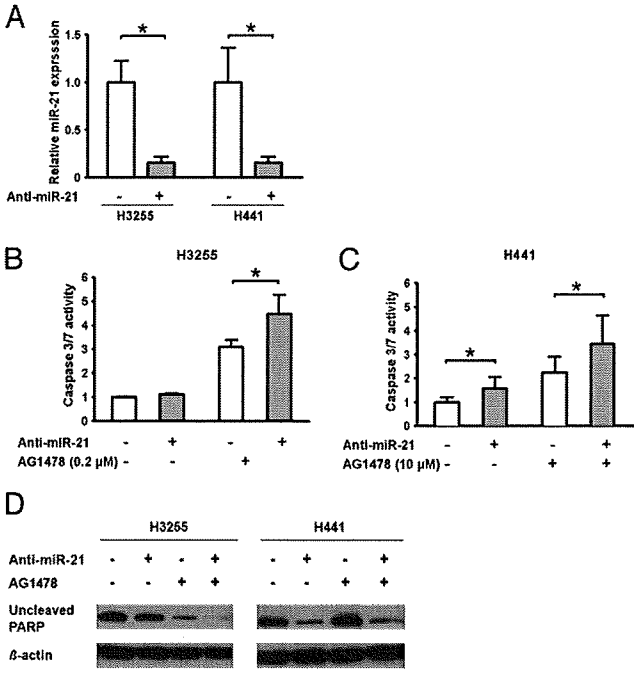

Fig. 3. Inhibition of miR-21 enhances AG1478-induced apoptosis. (*A*) Cells were transfected with 40 nM of anti-miR-21 (+) or control oligonucleotide (anti-EGFP) (−) for 72 h and examined by qRT-PCR. The expression levels of miR-21 after transfection of anti-miR-21 were expressed as the relative values to control. Data were mean ± SD from 3 independent experiments. *, $P < 0.05$, paired *t*-test. (*B*, *C*) Cells (H3255 or H441) were transfected with 40 nM of anti-miR-21 (+) or anti-EGFP (−) for 72 h and then were grown in the presence or absence of 0.2 μM of AG1478 for 24 h (H3255) or 10 μM for 72 h (H441). The activities of caspase 3/7 were expressed as the values relative to the activities of cells without anti-miR-21 and AG1478. Data were mean ± SD from at least 4 independent experiments. *, $P < 0.05$, Student's *t*-test. (*D*) Uncleaved PARP was evaluated by Western blot analysis. Cells were transfected with anti-miR-21 or anti-EGFP as described previously and then were grown in the presence or absence of 2 μM of AG1478 for 72 h. β-actin was a loading control.

Discussion

This study shows molecular characteristics of lung cancers in never-smokers and smokers: (*i*) changes in expression of a relatively small number of miRNAs are involved in lung carcinogenesis in never-smokers; (*ii*) *EGFR* mutations may reinforce some of these changes in miRNA expression, e.g., an increase in miR-21; (*iii*) miR-138 on 3p21.33, a chromosomal region carrying a long-sought lung cancer suppressor gene, is down-regulated preferentially in never-smoker cases; and (*iv*) miR-21 is one of the most aberrantly increased miRNAs in both never-smoker and smoker cases. There was no significant difference in the expression levels of miR-21 when stage I cases (n = 21) were compared with stage II, III, and IV cases (n = 7) (data not shown), suggesting that increased miR-21 expression is an early event in lung carcinogenesis. These findings identified miR-21 as a major miRNA that may play an oncogenic role in lung carcinogenesis and prompted us to choose it as a candidate for molecular targets in treatment of lung cancers in never-smokers as well as in smokers. Given the relationship between *EGFR* mutations and miR-21 up-regulation, we also hypothesized that this miRNA might have implications in improving EGFR-TKI therapy, whose effectiveness is correlated with *EGFR* gene status and smoking history of the patients (2, 4–6, 31).

Although high levels of miR-21 expression have been reported in various types of human tumors (19, 30, 32), including lung cancer from both smokers (18) and never-smokers (this study), the mechanism that up-regulates miR-21 during carcinogenesis is not well understood. In addition to the miRNA microarray data showing higher levels of miR-21 in *EGFR*-mutant cases (Table 3), the in vitro analyses using NSCLC cell lines showed that the activated EGFR signaling up-regulates miR-21 expression. A statistically significant positive correlation was observed between miR-21 expression levels and *p*-EGFR levels in NSCLC cell lines (Fig. 1*B*). Furthermore, the treatment with the EGFR-TKI (AG1478) inhibited miR-21 expression in 2 NSCLC cell lines with elevated *p*-EGFR, *EGFR*-mutant H3255 (Fig. 2) and *EGFR* wild-type H441 (Fig. S4), providing a mechanistic link between the activated EGFR signaling pathway and the aberrant up-regulation of miR-21 and a therapeutic basis for inhibition of miR-21 in lung cancers with EGFR activation. STAT3 reportedly signals IL-6–induced up-regulation of miR-21 in multiple myeloma cells (33). However, siRNA-mediated knockdown of endogenous STAT3 expression did not affect miR-21 levels in H441, H1650, and H1975 cells (data not shown), suggesting that STAT3 does not play a primary role in the EGFR signaling-induced up-regulation of miR-21 in NSCLC cells. It remains to be examined whether activator protein-1 (AP-1), which is activated by the EGFR signaling (34) and activates the miR-21 transcription through the binding to the promoter (35), is responsible for the increased expression of miR-21 in NSCLC cells. Nevertheless, there also should be EGFR-independent mechanisms to control miR-21 expression, because miR-21 was expressed abundantly in A549 cells without *EGFR* mutation or *p*-EGFR (Figs. 1*A* and S3*B*), and no increased miR-21 expression was observed in H1650 cells with *EGFR* mutation and increased *p*-EGFR (Figs. 1*A* and S3*C*). An increased copy number or amplification of the chromosomal region carrying *miR-21* (17q23.1) (36) may be an EGFR-independent mechanism.

Antisense oligonucleotide-mediated knockdown of miR-21 induced or enhanced apoptotic responses in 2 NSCLC cell lines, H3255 and H441 (Fig. 3) probably recapitulating some lung cancer cases from never-smokers. H3255 and H441 both expressed elevated levels of miR-21 (Fig. 1*A*) but had biologically and genetically different features. H3255 was highly responsive to EGFR-TKI (Fig. 1*A*), expressed high levels of *p*-EGFR (Figs. 2*A* and S3*C*), and had mutated and amplified *EGFR* (Fig. 1*A*) (37). H441 was less responsive to EGFR-TKI (Fig. 1*A*), expressed low levels of *p*-EGFR (Fig. S3*B*), and had wild-type *EGFR* (Fig. 1*A*). As previously reported in other types of human cancer cells (32, 33), the antisense inhibition of miR-21 by itself led to increased apoptotic response in H441 cells (Fig. 3 *C* and *D*), suggesting that miR-21 also can be a therapeutic target in lung cancers. Importantly, in both cell lines, anti-miR-21 significantly enhanced the apoptotic response induced by AG1478 (Fig. 3 *B* and *C*). The lack of effect of anti-miR-21 alone in H3255 cells (Fig. 3*B*) may indicate that the combinational use of anti-miR-21 and EGFR-TKI is required to attenuate effectively the constitutively activated EGFR signaling pathway to cell survival, which is evidenced by the highest levels of *p*-EGFR (Fig. S3*C*) and miR-21 (Fig. 1*A*). Although EGFR-TKIs are in wide clinical use for lung cancer (38), and inhibition of oncogenic miRNAs is a new promising approach in cancer therapy (39), this study reveals that the combination of these 2 therapeutic strategies can be significantly more effective than either alone. The finding is of particular importance in developing better treatment for lung cancer patients of non-Asian ethnicity, who tend to be less responsive to the current EGFR-TKI therapy (40). This study also has potential clinical implications in preventing and rescuing acquired EGFR-TKI resistance in NSCLC, an issue with important clinical relevance. Besides a secondary T790M mutation (41) and acquired MET amplification (42), selection of an *EGFR* wild-type subpopulation on a background of wild-type/mutant mixture leads to acquired EGFR-TKI resistance in NSCLC (43). The combinatorial use of EGFR-TKI and anti-miR-21 could prevent and rescue such acquired resistance caused by the selection for wild-type *EGFR*, because anti-miR-21 is effective on both *EGFR* wild-type and mutant tumor cells. Successful i.v. administration of a locked nucleic acid-modified antisense miRNA in primates (44) supports the feasibility of in vivo targeting miRNAs in therapy of human diseases.

Last, our lists of dysregulated miRNAs (Tables 2 and 3) include a number of other miRNAs that may have an oncogenic or tumor-suppressive role in lung carcinogenesis, e.g., up-regulated miR-141 (45), up-regulated miR-210 (46), down-regulated miR-126 (47), and down-regulated miR-486 (48). Further studies will address the roles of other individual miRNAs in lung carcinogenesis and a possible therapeutic relevance of overexpression and/or knockdown of multiple miRNAs.

In conclusion, lung cancers in never-smokers have a characteristic profile of miRNA expression. MiR-21 is a downstream effector of the activated EGFR signaling pathway and can be a therapeutic target in lung cancers with and without *EGFR* mutations. Antisense inhibition of miR-21 may improve clinical response to EGFR-TKI therapy.

Materials and Methods

Clinical Samples and Cell Lines. Lung cancer tissues and corresponding noncancerous tissues were obtained from never-smokers who had undergone surgical resection between 2000 and 2004 at the University of Maryland Medical Center (n = 15) or the Mayo Clinic (n = 7) in United States or at the Hamamatsu University School of Medicine (n = 6) in Japan (Tables 1 and S1). Institutional review board approval and written informed consent from all patients were obtained at each collection site. H3255 was provided by Dr. Bahar of the National Cancer Institute. A549, H23, H441, H1650, H1975, H157, and H1299 were purchased from American Type Culture Collection (ATCC). *hTERT*-immortalized normal human bronchial epithelial cells (HBET2) were established in our laboratory.

Microarray Analysis. Microarray analysis was performed as previously described (21, 49). Briefly, 5 μg of total RNA was used for hybridization on miRNA microarray chips containing 389 probes in triplicate (Ohio State microRNA microarray version 3.0). Processed slides were scanned using a PerkinElmer ScanArray XL5K Scanner. With statistical software R (http://www.r-project.org/), only spot values that were not flagged by the image quantification software GenePix Pro 6.0.1.00 (www.moleculardevices.com/pages/software/gn_genepix_pro.html) and whose foreground intensities were larger than background intensities were used. The remaining spots then were normalized by locally weighted scatterplot smoothing (LOESS), and duplicate spots were averaged. The preprocessed and normalized data then were imported into BRB-ArrayTools version 3.5.0 (http://linus.nci.nih.gov/BRB-ArrayTools.html). Finally, 291 miRNAs with non-missing log values present in more than 75% of the samples were selected. More information is available in *SI Materials and Methods*.

Real-Time RT-PCR Analysis. Expression of mature miRNAs was examined by qRT-PCR analysis using a TaqMan Human MicroRNA Assay kit and a PRISM 7700 Sequence Detector System (Applied Biosystems). RNU6B was an endogenous control (#4373381, Applied Biosystems). Gene expression data (mean ± SD from triplicate samples) were shown as $2^{-\Delta\Delta CT}$ (50).

Cell Treatment and Growth Inhibition Assay. To evaluate the effect of AG1478 on the EGFR signaling pathway and miR-21 expression levels, lung cancer cell lines were serum starved for 24 h, incubated in the presence or absence of AG1478 (2 μM or 10 μM; Calbiochem) for 2 h, and then for an additional 15 min in the presence or absence of EGF (20 ng/mL; Promega). Growth inhibition was assessed by 3-(4,5-dimethylthiazol-2-yl)-5-(3-carboxymethoxyphenyl)-2-(4-sulfophenyl) 2H-tetrazolium, inner salt (MTS) assay (Dojindo). Cells (5,000/well) were seeded into 96-well plates, and increasing concentrations of AG1478 (0, 0.4, 2.0, 10, and 50 μM) were added. After incubation for 72 h at 37 °C, MTS was added and incubated for 2 h at 37 °C; then absorbance at 450 nm was measured. The IC_{50} value was defined as the concentration needed for 50% reduction of the growth.

Western Blot Analysis. Cells were lysed in buffer containing 50 mM Tris-HCl, pH 7.6, 150 mM NaCl, 0.1% SDS, 1% Nonidet P-40, and 0.5% sodium-deoxycholate. Ten μg of proteins were separated by gel electrophoresis on 10% gels, transferred to nitrocellulose membranes, and detected by immunoblotting using a chemiluminescence system (GE Healthcare Bio-Sciences Corp.). The images were quantified using National Institutes of Health ImageJ1.40g (http://rsb.info.nih.gov/ij/). Antibodies are in *SI Materials and Methods*.

Oligonucleotide Transfection and Apoptosis Assay. Cells were transfected with the oligonucleotides (at a final concentration of 40 nM) using LipofectAMINE 2000 reagent (Invitrogen). After 72 h, the cells were incubated in the presence or absence of 0.2 μM of AG1478 for 24 h (H3255) or 10 μM of AG1478 for 72 h (H441). Activities of caspase-3 and caspase-7 were analyzed using ApoONE Homogeneous Caspase 3/7 Assay (Promega). Each experiment was done in triplicate and at least 4 times independently. The data were shown as mean ± SD. Oligonucleotide sequences are in *SI Materials and Methods*.

Statistical Analysis. The paired *t*-test identified miRNAs that were differentially expressed in lung cancer tissues and normal lung tissues ($P < 0.01$, FDR < 0.15). We also identified miRNAs that were differently expressed in *EGFR*-mutant and wild-type lung cancers using the F-test ($P < 0.01$, FDR < 0.15). The paired *t*-test was used to analyze differences in miRNA expression in tumors and corresponding normal tissues for qRT-PCR data. Graphpad Prism v5.0 (Graphpad Software Inc.) analysis was used for the Pearson's correlation. All statistical tests were 2-sided, and statistical significance was defined as $P < 0.05$.

ACKNOWLEDGMENTS. We thank Dr. Kensuke Kumamoto for helpful discussions, Drs. Raymond T. Jones, Andrew Borkowski, and Mark J. Krasna for sample collection and pathology reports, and Audrey Salabes for interviewing the lung cancer patients. This work was supported by the Intramural Research Program of the National Institutes of Health, National Cancer Institute, and Center for Cancer Research.

1. Parkin DM, Bray F, Ferlay J, Pisani P (2005) Global cancer statistics, 2002. *CA Cancer J Clin* 55:74–108.
2. Mountzios G, Fouret P, Soria JC (2008) Mechanisms of disease: Signal transduction in lung carcinogenesis—a comparison of smokers and never-smokers. *Nature Clinical Practice Oncology* 5:610–618.
3. Hollstein M, Sidransky D, Vogelstein B, Harris CC (1991) p53 mutations in human cancers. *Science* 253:49–53.
4. Vähäkangas KH, et al. (2001) p53 and *K-ras* mutations in lung cancers from former and never-smoking women. *Cancer Res* 61:4350–4356.
5. Mounawar M, et al. (2007) Patterns of *EGFR*, *HER2*, *TP53*, and *KRAS* mutations of $p14^{arf}$ expression in non-small cell lung cancers in relation to smoking history. *Cancer Res* 67:5667–5672.
6. Sun S, Schiller JH, Gazdar AF (2007) Lung cancer in never smokers—a different disease. *Nature Reviews Cancer* 7:778–790.
7. Lynch TJ, et al. (2004) Activating mutations in the epidermal growth factor receptor. *N Engl J Med* 350:2129–2139.
8. Paez JG, et al. (2004) EGFR mutations in lung cancer: Correlation with clinical response to gefitinib therapy. *Science* 304:1497–1500.
9. Uramoto H, Mitsudomi T (2007) Which biomarker predicts benefit from EGFR-TKI treatment for patients with lung cancer? *Br J Cancer* 96:857–863.
10. Calin GA, et al. (2002) Frequent deletions and down-regulation of micro-RNA genes *miR15* and *miR16* at 13q14 in chronic lymphocytic leukemia. *Proc Natl Acad Sci USA* 99:15524–15529.
11. Inamura K, et al. (2007) let-7 microRNA expression is reduced in bronchioloalveolar carcinoma, a non-invasive carcinoma, and is not correlated with prognosis. *Lung Cancer* 58:392–396.
12. Lu J, et al. (2005) MicroRNA expression profiles classify human cancers. *Nature* 435:834–838.
13. Calin GA, et al. (2005) A microRNA signature associated with prognosis and progression in chronic lymphocytic leukemia. *N Engl J Med* 353:1793–1801.
14. Volinia S, et al. (2006) A microRNA expression signature of human solid tumors defines cancer gene targets. *Proc Natl Acad Sci USA* 103:2257–2261.
15. Johnson SM, et al. (2005) RAS is regulated by the let-7 microRNA family. *Cell* 120:635–647.
16. Takamizawa J, et al. (2004) Reduced expression of the let-7 microRNAs in human lung cancers in association with shortened postoperative survival. *Cancer Res* 64:3753–3756.
17. Hayashita Y, et al. (2005) A polycistronic microRNA cluster, miR-17–92, is overexpressed in human lung cancers and enhances cell proliferation. *Cancer Res* 65:9628–9632.
18. Yanaihara N, et al. (2006) Unique microRNA molecular profiles in lung cancer diagnosis and prognosis. *Cancer Cell* 9:189–198.
19. Schetter AJ, et al. (2008) MicroRNA expression profiles associated with prognosis and therapeutic outcome in colon adenocarcinoma. *J Am Med Assoc* 299:425–436.
20. Weidhaas JB, et al. (2007) MicroRNAs as potential agents to alter resistance to cytotoxic anticancer therapy. *Cancer Res* 67:11111–11116.
21. Liu CG, Calin GA, Volinia S, Croce CM (2008) MicroRNA expression profiling using microarrays. *Nature Protocols* 3:563–578.
22. Landi MT, et al. (2008) Gene expression signature of cigarette smoking and its role in lung adenocarcinoma development and survival. *PLoS ONE* 20:e1651.
23. Ding L, et al. (2008) Somatic mutations affect key pathways in lung adenocarcinoma. *Nature* 455:1069–1075.
24. Zabarovsky ER, Lerman MI, Minna JD (2002) Tumor suppressor genes on chromosome 3p involved in the pathogenesis of lung and other cancers. *Oncogene* 21:6915–6935.
25. Mitomo S, et al. (2008) Downregulation of miR-138 is associated with overexpression of human telomerase reverse transcriptase protein in human anaplastic thyroid carcinoma cell lines. *Cancer Sci* 99:280–286.
26. Horikawa I, Barrett JC (2003) Transcriptional regulation of the telomerase *hTERT* gene as a target for cellular and viral oncogenic mechanisms. *Carcinogenesis* 24:1167–1176.
27. Sharma SV, Bell DW, Settleman J, Haber DA (2007) Epidermal growth factor receptor mutations in lung cancer. *Nat Rev Cancer* 7:169–181.
28. Tracy S, et al. (2004) Gefitinib induces apoptosis in the $EGFR^{L858R}$ non-small-cell lung cancer cell line H3255. *Cancer Res* 64:7241–7244.
29. Sordella R, Bell DW, Haber DA, Settleman J (2004) Gefitinib-sensitizing EGFR mutations in lung cancer activate anti-apoptotic pathways. *Science* 305:1163–1167.
30. Meng F, et al. (2007) MicroRNA-21 regulates expression of the PTEN tumor suppressor gene in human hepatocellular cancer. *Gastroenterology* 133:647–658.
31. Toyooka S, et al. (2007) The impact of sex and smoking status on the mutational spectrum of epidermal growth factor receptor gene in non small cell lung cancer. *Clin Cancer Res* 13:5763–5768.
32. Chan JA, Krichevsky AM, Kosik KS (2005) MicroRNA-21 is an antiapoptotic factor in human glioblastoma cells. *Cancer Res* 65:6029–6033.
33. Löffler D, et al. (2007) Interleukin-6 dependent survival of multiple myeloma cells involves the Stat3-mediated induction of microRNA-21 through a highly conserved enhancer. *Blood* 110:1330–1333.
34. Li J, et al. (2003) Differential requirement of EGF receptor and its tyrosine kinase for AP-1 transactivation induced by EGF and TPA. *Oncogene* 22:211–219.
35. Fujita S, et al. (2008) miR-21 Gene expression triggered by AP-1 is sustained through a double-negative feedback mechanism. *J Mol Biol* 378:492–504.
36. Łastowska M, et al. (2002) Breakpoint position on 17q identifies the most aggressive neuroblastoma tumors. *Genes Chromosomes Cancer* 34:428–436.
37. Engelman JA, et al. (2006) Allelic dilution obscures detection of a biologically significant resistance mutation in EGFR-amplified lung cancer. *J Clin Invest* 116:2695–2706.
38. Shepherd FA, et al. (2005) Erlotinib in previously treated non-small-cell lung cancer. *N Engl J Med* 353:123–132.
39. Bumcrot D, Manoharan M, Koteliansky V, Sah DW (2006) RNAi therapeutics: A potential new class of pharmaceutical drugs. *Nat Chem Biol* 2:711–719.
40. Thatcher N, et al. (2005) Gefitinib plus best supportive care in previously treated patients with refractory advanced non-small-cell lung cancer: Results from a randomised, placebo-controlled, multicentre study (Iressa Survival Evaluation in Lung Cancer). *Lancet* 366:1527–1537.
41. Kobayashi S, et al. (2005) EGFR mutation and resistance of non-small-cell lung cancer to gefitinib. *N Engl J Med* 24:786–792.
42. Engelman JA, et al. (2007) MET amplification leads to gefitinib resistance in lung cancer by activating ERBB3 signaling. *Science* 316:1039–1043.
43. Jiang SX, et al. (2008) EGFR genetic heterogeneity of nonsmall cell lung cancers contributing to acquired gefitinib resistance. *Int J Cancer* 123:2480–2486.
44. Elmén J, et al. (2008) LNA-mediated microRNA silencing in non-human primates. *Nature* 452:896–899.
45. Iorio MV, et al. (2007) MicroRNA signatures in human ovarian cancer. *Cancer Res* 67:8699–8707.
46. Foekens JA, et al. (2008) Four miRNAs associated with aggressiveness of lymph node-negative, estrogen receptor-positive human breast cancer. *Proc Natl Acad Sci USA* 105:13021–13026.
47. Liu B, et al. (2009) MiR-126 restoration down-regulate VEGF and inhibit the growth of lung cancer cell lines in vitro and in vivo. *Lung Cancer*, in press.
48. Gal H, et al. (2008) MIR-451 and imatinib mesylate inhibit tumor growth of glioblastoma stem cells. *Biochem Biophys Res Commun* 376:86–90.
49. Liu CG, et al. (2004) An oligonucleotide microchip for genome-wide microRNA profiling in human and mouse tissues. *Proc Natl Acad Sci USA* 101:9740–9744.
50. Schmittgen TD, et al. (2008) Real-time PCR quantification of precursor and mature microRNA. *Methods* 44:31–38.

Lung Cancer xxx (2009) xxx–xxx

Contents lists available at ScienceDirect

Lung Cancer

journal homepage: www.elsevier.com/locate/lungcan

Expression of RACK1 is a novel biomarker in pulmonary adenocarcinomas

Ryo Nagashio[a,b], Yuichi Sato[b,c,*], Toshihide Matsumoto[c], Taihei Kageyama[c], Yukitoshi Satoh[d], Ryuge Shinichiro[e], Noriyuki Masuda[e], Naoki Goshima[g], Shi-Xu Jiang[c,f], Isao Okayasu[c,f]

[a] Division of Pathology, National Cancer Center Research Institute, Tokyo, Japan
[b] Department of Molecular Diagnostics, School of Allied Health Sciences, Kitasato University, Kanagawa, Japan
[c] Department of Cellular and Histo-Pathology, Graduate School of Medical Sciences, Kitasato University, Kanagawa, Japan
[d] Department of Thoracic and Cardiovascular Surgery, School of Medicine, Kitasato University, Kanagawa, Japan
[e] Department of Respiratory Medicine, School of Medicine, Kitasato University, Kanagawa, Japan
[f] Department of Pathology, School of Medicine, Kitasato University, Kanagawa, Japan
[g] National Institute of Advanced Industrial Science and Technology (AIST), Tokyo, Japan

ARTICLE INFO

Article history:
Received 4 April 2009
Received in revised form 5 August 2009
Accepted 29 September 2009

Keywords:
Lung cancer
Receptor of activated C kinase 1
Immunization methodology
Monoclonal antibody
Two-dimensional electrophoresis
Immunoblotting
Immunohistochemistry

ABSTRACT

To develop useful early and/or differential diagnostic markers for pulmonary adenocarcinomas, we generated monoclonal antibodies using A549 cells derived from pulmonary adenocarcinomas as an immunogen. Hybridoma supernatants were immunohistochemically screened for antibody production by AMeX-fixed and paraffin-embedded A549 cell preparations. Positive clones were monocloned twice by limiting dilutions. From a group of obtained antibodies, an antibody designated as KU-Lu-3 showed cytoplasmic staining. The antigen recognized by KU-Lu-3 was detected by modified two-dimensional immunoblotting, and was determined to be the receptor of activated C kinase 1 (RACK1). To evaluate the utility of KU-Lu-3, we immunohistochemically studied 184 cases of pulmonary carcinoma and paired normal lung tissues, using formalin-fixed and paraffin-embedded tissue microarray sections. The expression was significantly high and frequent in adenocarcinomas but was barely detected in a few squamous cell carcinomas and large cell carcinomas ($p < 0.0001$). Moreover, RACK1 expression was also significantly associated with the pathological stage, tumor size and lymph node status of adenocarcinoma patients, but not with tumor differentiation, or patient age and gender. These results suggest that RACK1 may be a novel differential diagnostic marker for pulmonary adenocarcinomas.

1. Introduction

Lung cancer is the leading cause of cancer-related death, but the 5-year overall survival rate is still below 16% [1]. Non-small cell lung carcinomas (non-SCLC) account for almost 80% of lung cancers, of which 50% are adenocarcinomas (AD). Although the overall 5-year survival rate of patients diagnosed in stage I AD is about 63%, nearly 35% will relapse after surgical resection. Identification of these high-risk patients with resectable early-stage disease would provide the opportunity for adjuvant therapy, possibly leading to increased survival, therefore, the acquisition of markers to diagnose AD earlier and to identify high-risk patients with AD is anticipated.

Antibodies are mainly developed using purified proteins or synthetic peptides. We have generated monoclonal antibodies (MoAbs) exhaustively against various tumor-associated proteins using pulmonary AD-derived A549 cells as an immunogen, namely, the random immunization method [2]. This method is expected to obtain antibodies against tumor-specific proteins with post-translational modifications, which are difficult to obtain by conventional immunization methods.

Receptor of activated C kinase (RACK1) is a 36 kDa cytosolic protein with a propeller-like structure of seven WD40 repeats and belongs to a WD40 superfamily of proteins, including the β subunit of G-proteins [3]. The WD40 repeats of RACK1 play a role in complex protein–protein interactions among signaling molecules such as β integrins, phosphodiesterase 4D5, and Src tyrosine kinase, as well as protein kinase C (PKC) [4–6]. RACK1 is likely to be essential for cellular functions because its amino acid sequence is 100% identical in humans, rats, chickens [3], mice [7], and cows [8], and RACK1

Abbreviations: 2DE, two-dimensional gel electrophoresis; AD, adenocarcinoma; ACN, acetonitrile; AEC, 3-amino-9-ethylcarbazole; CBB, Coomassie brilliant blue; FBS, fetal bovine serum; HCF, hybridoma cloning factor; IHC, immunohistochemical staining; LCC, large cell carcinoma; LCNEC, large cell neuroendocrine carcinoma; M.W., molecular weight; MoAb, monoclonal antibody; NSS, normal swine serum; PKC, protein kinase C; PVDF, polyvinylidene difluoride; RACK1, receptor of activated C kinase 1; RT, room temperature; SCC, squamous cell carcinoma; SCLC, small cell lung carcinoma; SDS-PAGE, sodium dodecyl sulfate-polyacrylamide gel electrophoresis; TTF-1, thyroid transcription factor 1; VEGF, vascular endothelial growth factor.

* Corresponding author at: Department of Molecular Diagnostics, School of Allied Health Sciences, Kitasato University, 1-15-1, Kitasato, Sagamihara, Kanagawa 228-8555, Japan. Tel.: +81 42 778 8013; fax: +81 42 778 9854.
E-mail address: yuichi@med.kitasato-u.ac.jp (Y. Sato).

0169-5002/$ – see front matter © 2009 Elsevier Ireland Ltd. All rights reserved.
doi:10.1016/j.lungcan.2009.09.015

Please cite this article in press as: Nagashio R, et al. Expression of RACK1 is a novel biomarker in pulmonary adenocarcinomas. Lung Cancer (2009), doi:10.1016/j.lungcan.2009.09.015

is ubiquitously expressed in a wide range of tissues, including the brain, liver, and spleen [3].

PKCβ plays an important role in vascular endothelial growth factor (VEGF)-mediated tumor development, not only at the initial stage of tumor development, but also after the tumor is fully established [9]. Furthermore, PKCβ plays an important role in cancer growth [9]. There are few reports concerning the expression of RACK1 and its association with tumor aggressiveness. Berns et al. reported that RACK1 messenger RNA expression was higher in non-SCLC and colon carcinomas than in the corresponding normal tissues [8]. To our knowledge, the expression of RACK1 protein in cancers, including lung cancer, has not been studied.

The present study demonstrates the methodology for exhaustive production of MoAbs and the utility of obtained KU-Lu-3 antibody recognizing RACK1 by immunohistochemical study with formalin-fixed and paraffin-embedded tissue microarray sections of 184 lung cancers and their normal tissues.

2. Materials and methods

2.1. Cell lines

A549 cells, derived from a lung AD, were purchased from the Japanese Cancer Research Resources Bank (Tokyo, Japan) and grown in RPMI-1640 medium (SIGMA, Steinheim, Germany) supplemented with 10% fetal bovine serum (FBS; Biowest, Miami, FL), 100 units/ml penicillin, and 100 μg/ml streptomycin (PS; Gibco, Auckland, New Zealand). SP2/O cells, derived from a mouse myeloma, were grown in RPMI-1640 medium supplemented with 1× 8-azaguanine (50× Hybri-Max, SIGMA), 10% FBS, and PS. After harvesting and washing twice with phosphate-buffered saline without bivalent ions (PBS-), subconfluented A549 cells were AMeX-fixed [10] for immunohistochemical screening or stored at −80 °C until used for immunization.

2.2. Tissues

A tissue microarray of 184 continuous cases of paired lung cancers and their normal lung tissues, surgically resected at Kitasato University Hospital, were fixed in 10% formalin and embedded in paraffin. Their tumors consisted of 123 ADs, 44 squamous cell carcinomas (SCCs), 4 large cell carcinomas (LCCs), 7 small cell carcinomas (SCLCs), and 6 large cell neuroendocrine carcinomas (LCNECs), and were prepared according to the protocol of Tissue Microprocessor KIN-type 1 (Azumaya, Tokyo, Japan). The patients were 125 men and 59 women, with a mean age of 65.5 years (range: 41–85 years) at the time of the initial visit.

This study was approved by the Ethics Committee of Kitasato University School of Medicine. All patients were informed of the aim of the study and gave consent to donate their samples.

2.3. Production of monoclonal antibodies

A549 cell lysate was prepared with PBS(−) using an ultra-sonic homogenizer (UH-50; SMT Company, Tokyo, Japan). Five-week-old female BALB/c mice were immunized intra-peritoneally with 50 mg wet weight of A549 cell lysate in 500 μl PBS(−) 3 times at two-week intervals. The antibody titer was tested by immunohistochemical staining (IHC) using 100-times diluted sera from immunized mice as the first antibody on AMeX-fixed A549 cells. Three days prior to cell fusion, the animal with the highest titer was intra-peritoneally boosted by the same A549 lysates, and hybridomas were produced as previously described [2]. The hybridoma screening involved IHC with AMeX-fixed cell preparations. Three-micrometer-thick sections of AMeX-fixed cell preparations were deparaffinized in xylene and rehydrated in descending ethanol series, and treated with 3% hydrogen peroxide for 10 min. After blocking with 2% normal swine serum (NSS; Nichirei, Tokyo, Japan) for 10 min, the sections were reacted with non-diluted hybridoma supernatants as the first antibody for 2 h at RT. After rinsing in TBS (0.01 M Tris–HCl pH 7.5, 150 mM NaCl) 3 times for 5 min each, the sections were reacted with ChemMate ENVISION reagent (Dako, Glostrup, Denmark) for 30 min at RT. Finally, the sections were visualized by Stable DAB solution (Invitrogen, Carlsbad, CA) and counterstained with Mayer's hematoxylin.

2.4. Sodium dodecyl sulfate-polyacrylamide gel electrophoresis (SDS-PAGE)

Proteins were extracted from A549 cells with detergent lysis buffer [11] using an ultra-sonic homogenizer (UH-50; SMT Company, Tokyo, Japan). Ten micrograms of extracted proteins were boiled and separated by SDS-PAGE with 12% polyacrylamide gel with a constant current at 20 mA.

2.5. Agarose two-dimensional gel electrophoresis (2DE)

Solubilization of cells and quantification of cell lysates were described previously in our paper [12]. The Agarose-2DE method used in this study was also previously described [12]. Two pieces of gel were prepared for one sample; one was transferred to a polyvinylidene difluoride (PVDF) membrane (MILLIPORE Corp., Bedford, MA) for immunoblotting and another was visualized by Coomassie brilliant blue R-350 (CBB, PhastGel Blue R; Amersham Pharmacia Biotech AB, Uppsala, Sweden) staining.

2.6. Immunoblotting

Blotting membranes were blocked with ImmunoBlock (Dainippon Sumitomo Pharma, Osaka, Japan) for 1 h at RT. The membranes were then reacted with non-diluted hybridoma supernatants for 2 h at RT, and incubated with 1000-times diluted horseradish peroxidase conjugated rabbit anti-mouse IgG polyclonal antibody (Dako) with 2% NSS for 30 min at RT. Finally, signals were developed by Immobilon Western (MILLIPORE Corp.) for 1D immunoblotting and 3-amino-9-ethylcarbazole (AEC) substrate (Dako) for 2D immunoblotting. The immunoblot membrane visualized in AEC was further stained with amidoblack to confirm the corresponding protein spot with CBB-stained 2DE gel. Both staining images were taken with a high-resolution scanner (GT-9800; EPSON, Tokyo, Japan), and the equivalent positive spot was cut out.

2.7. Identification of antigen protein

2.7.1. In gel digestion

In brief, protein spots were excised from a 2DE gel, destained with 50% (v/v) acetonitrile (ACN)/50 mM NH_4HCO_3, dehydrated with 100% (v/v) ACN, and dried under vacuum conditions. Tryptic digestion was performed for 24 h at 37 °C in a minimum volume of digestion solution which contained 20 ng/μl trypsin (Trypsin Gold, Mass Spectrometry Grade, Promega, Madison, WI) and 25 mM NH_4HCO_3. After incubation, digested protein fragments eluted in solution were collected, and gels were washed once in 5% (v/v) trifluoroacetic acid/50% (v/v) ACN and collected in the same tube.

2.7.2. On membrane digestion

AEC-stained spots were excised from the PVDF membrane, stripped and re-probed using Restore™ Western Blot Stripping Buffer (PIERCE, Rockford, IL) for 15 min at RT, and destained with 50% (v/v) ACN/50 mM NH_4HCO_3 for 30 min. The membrane pieces

Please cite this article in press as: Nagashio R, et al. Expression of RACK1 is a novel biomarker in pulmonary adenocarcinomas. Lung Cancer (2009), doi:10.1016/j.lungcan.2009.09.015

were dried under vacuum conditions, and then treated and collected using the same methods as for gel digestion.

2.7.3. Protein identification

Tryptic peptides were spotted on a Prespotted AnchorChip 96 Set for Proteomics (Bruker Daltonik GmbH, Bremen, Germany) according to the manufacturer's recommendations. MS spectra were analyzed in an autoflex III TOF/TOF (Bruker Daltonik GmbH) in reflector mode by summarizing 1000 signal spectra (5 × 200) with a 50 Hz laser in the mass range from 580 to 4000 Da applying the following instrument settings; ion source 1: 19.00 kV, ion source 2: 16.60 kV, lens: 8.55 kV, reflector 1: 21.00 kV, reflector 2: 9.70 kV, reflector detector: 1400 V, suppression up to 500 Da by deflection.

Then, MS/MS spectra of tryptic peptides were further measured in an Autoflex III TOF/TOF in MS/MS mode using the following instrument settings: ion source 1: 6.00 kV, ion source 2: 5.30 kV, lens: 3.00 kV, reflector 1: 27.00 kV, reflector 2: 11.65 kV, lift 1: 19.00 kV, lift 2: 4.20 kV, reflector detector: 1400 V.

Fragment ion spectra from MS and MS/MS were submitted to MASCOT (http://www.matrixscience.com/) for a database search and the identification of corresponding proteins employing the following database: IPI human 20081114 (74049 sequences; 31194560 residues, http://www.ebi.ac.uk/IPI/IPIhuman.http://www.ebi.ac. uk/IPI/IPIhuman.html/).

2.7.4. Immunohistochemical staining

Formalin-fixed and paraffin-embedded tissue sections were immunostained in the same way as described in AMeX-fixed cell preparations in addition to antigen retrieval by autoclaving in 0.01 M citrate buffer (pH 6.0) with 0.1% Tween 20 at 121 °C for 10 min.

IHC for thyroid transcription factor 1 (TTF-1) expression was performed in the same way as described for RACK1 using TTF-1 antibody (8G7G3/1, Dako, 1/200 dilution).

2.7.5. Evaluation of IHC

RACK1 was scored by multiplication of the percentage of positive tumor cells and staining intensity [12]. The percentage of positive tumor cells was scored as 0 (0%), 1+ (1–25%), 2+ (26–50%), 3+ (51–75%), or 4+ (76–100%). Staining intensity was also scored as 1+ (weakly positive), 2+ (moderately positive), or 3+ (strongly positive).

Regarding TTF-1 staining, to exclude equivocal reactions, an at least moderate intensity in more than 10% of the tumor cells was considered as positive staining.

The Mann–Whitney *U*-test was used for statistical evaluation of IHC data. $p < 0.05$ was considered significant.

3. Results

3.1. Confirmation of antibody titer in mice sera and production of MoAbs

The antibody titer was tested by immunohistochemical staining using 100-times diluted sera of immunized mice as the first antibody on AMeX-fixed A549 cells. As a result, the sera of immunized mice contained antibodies that reacted with various cell components (Fig. 1).

Using AMeX-fixed A549 cell preparations for immunohistochemical screening, we finally obtained 188 MoAbs. An antibody, designated KU-Lu-3, which showed strong cytoplasmic staining on A549 cells, was picked up and further studied.

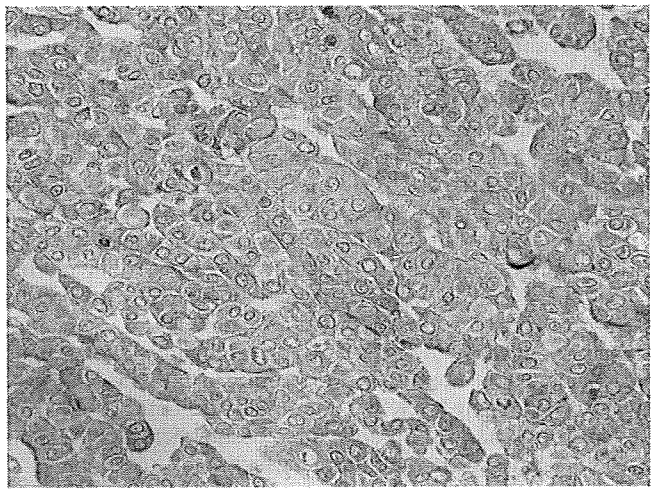

Fig. 1. The antibody titer was tested immunohistochemically using 100-times diluted sera of immunized mice as a first antibody on AMeX-fixed A549 cells used as an immunogen. The sera of immunized mice contained antibodies that reacted with various cell components, such as cytoplasmic proteins and plasma membranes.

3.2. One-dimensional (1D) immunoblot analysis with hybridoma supernatant

1D immunoblot analysis of cell lysate from A549 cells using KU-Lu-3 supernatant as the first antibody was performed. This antibody was recognized as a roughly 29 kDa protein (Fig. 2).

3.3. Identification of antigenic protein by two-dimensional (2D) immunoblotting

In order to purify and identify the protein which was recognized by KU-Lu-3 antibody, we performed 2DE with lysate from A549 cells, followed by immunoblot analysis using the supernatant of KU-Lu-3 antibody as the primary antibody. The result of 2D immunoblot is shown in Fig. 3. The antigenic protein showed a rough molecular weight (M.W.) of 29 kDa and isoelectric point of 7.5–8.5. To identify the protein recognized by KU-Lu-3 antibody, we cut out the spot from the 2D gel and membrane, and proceeded with in gel and on membrane digestion, respectively. After analysis by matrix-assisted laser desorption time-of-flight/time-of-flight mass spectrometry and MASCOT search, the protein was determined as a receptor of activated C kinase 1 (RACK1, accession: P63244), which is composed of 316 amino acids with a predicted M.W. of 34,946 Da and theoretic isoelectric point of 7.90.

3.4. IHC of RACK1

To evaluate the utility of KU-Lu-3 as diagnostic marker, we studied IHC using the tissue microarray of pulmonary carcinomas and their normal lung tissues. Staining results are summarized in Table 1. The expression of RACK1 was localized in the cytoplasm

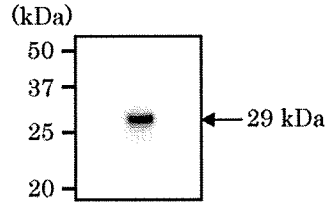

Fig. 2. Immunoblot analysis with whole cell lysate from A549 cell using hybridoma supernatant as the first antibody. The antibody recognized an approximately 29 kDa protein.

Please cite this article in press as: Nagashio R, et al. Expression of RACK1 is a novel biomarker in pulmonary adenocarcinomas. Lung Cancer (2009), doi:10.1016/j.lungcan.2009.09.015

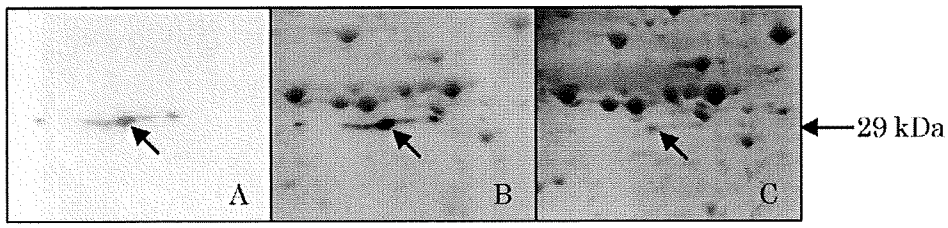

Fig. 3. 2D immunoblot analysis of KU-Lu-3 andtibody on A549 cells. A549 cell lysate was separated by 2DE in duplicate. (A) The 29 kDa protein was detected on the membrane. (B) Amidoblack staining was performed on the membrane after immunoblotting. (C) The 2DE protein pattern on gel after CBB staining. Arrows indicate the same antigen recognized by KU-Lu-3 antibody.

of tumor cells and scattered in normal bronchial epithelial cells (Fig. 4H); therefore, the stainability of normal bronchial epithelium was used as an internal control. Moreover proliferative bronchial epithelia tend to show a strong expression of RACK1 (Fig. 4D). RACK1 was detected in 77 of 123 (62.6%) ADs, 3 of 44 (6.8%) SCCs, 1 of 4 (25.0%) LCCs, 0 of 7 (0%) SCLCs, and 3 of 6 (50.0%) LCNECs, and their mean staining scores of RACK1 were 2.9, 0.1, 0.8, 0, and 1.9, respectively. The positive rate and mean staining score in AD were significantly higher than in SCC ($p < 0.0001$). As for LCNEC, half showed positive staining at various degrees in their cytoplasm. Although a few cases of SCC and LCC showed faintly cytoplasmic staining, no obvious staining was observed in other tumors (Fig. 4E and F).

The expression of TTF-1 was localized in the nucleus of tumor cells and type II pneumocytes as well as in Clara cells in normal lung tissue. TTF-1 was detected in 105 of 123 (85.4%) ADs, 1 of 44 (2.3%) SCCs, 2 of 4 (50.0%) LCCs, 5 of 7 (71.4%) SCLCs, and 0 of 6 (0%) LCNECs.

The relationship between RACK1 expression and clinicopathological characteristics in the 123 ADs is summarized in Table 2. The expression levels of RACK1 were significantly associated with the pathological stage ($p = 0.0042$), tumor size ($p = 0.0074$), and lymph node status ($p = 0.0009$), respectively. No significant association between the expression levels of RACK1 and mucin production or TTF-1 staining was observed.

4. Discussion

In this study, which aimed to identify useful differential diagnostic markers for pulmonary ADs, we generated monoclonal antibodies using A549 cells derived from a pulmonary AD as an immunogen. From a group of obtained antibodies, we identified the antigen recognized by this antibody with methods that combined two-dimensional immunoblotting and a mass spectrometer, and confirmed that this antibody recognized a certain epitope of RACK1. To evaluate the utility of this antibody against RACK1, we immunohistochemically studied 184 cases of lung cancer and their normal tissues using formalin-fixed and paraffin-embedded tissue microarray sections. As a result, a high staining score and positive rate were found in AD. Moreover, RACK1 expression was significantly associated with the pathological stage ($p = 0.0042$), tumor size ($p = 0.0074$), and lymph node status (0.0009) of AD patients. These results suggest that RACK1 is a useful differential diagnostic marker for AD compared to other histologic types of lung carcinoma. Further, RACK1 may be important as one of the prognostic factors in pulmonary adenocarcinoma. Further studies are needed to clarify the relationship between the expression of RACK1 and the outcome in patients with pulmonary adenocarcinoma.

RACK1 was originally identified based on its ability to bind to protein kinase C and transport its activated form to specific regions

Table 1
Expression of RACK1 in pulmonary carcinomas.

RACK1	n	Score	Positive rate (%)
AD	123	2.9*	77/123 (62.6)
SCC	44	0.1*	3/44 (6.8)
LCC	4	0.8	1/4 (25.0)
SCLC	7	0	0/7 (0)
LCNEC	6	1.9	3/6 (50.0)

* $p < 0.0001$, significant difference in mean score of immunohistochemistry.

Table 2
Relationship between RACK1 expression and clinicopathological characteristics of adenocarcinomas.

Characteristics	n	Positive rate (%)	Score	p-Value
Age				
<50	7	5/7 (71.0)	1.4	0.4339
≥50	116	72/116 (62.1)	3.0	
Gender				
Male	68	45/68 (66.2)	3.3	0.2156
Female	55	32/55 (58.2)	2.5	
AD subtype (WHO)				
Mixed pattern	69	42/69 (60.9)	2.6	
BAC	4	2/4 (50.0)	2.5	
Acinar	3	3/3 (100)	3.7	
Papillary	43	27/43 (62.8)	3.3	
Solid with mucin	4	3/4 (75.0)	4.3	
Differentiation				
Well	55	35/55 (63.6)	2.9	0.8625
Moderate/poor	68	42/68 (61.8)	3.0	
Pathological stage				
I	67	47/67 (70.1)	3.7	0.0042
II–IV	56	30/56 (53.6)	2.1	
Tumor size				
<3	58	41/58 (70.7)	3.9	0.0074
≥3	65	36/65 (55.4)	2.1	
Lymph node status				
Negative	78	54/78 (69.2)	3.7	0.0009
Positive	45	23/45 (51.1)	1.6	
Mucin				
Negative	79	44/79 (55.7)	2.7	0.1797
Positive	44	33/44 (75.0)	3.4	
TTF-1				
Negative	17	11/17 (64.7)	3.2	0.7595
Positive	106	66/106 (62.3)	2.9	
Pleural invasion				
Negative	65	41/65 (63.1)	2.8	0.9061
Positive	56	35/56 (62.5)	3.0	
NA*	2			
Lymphatic invasion				
Negative	35	18/35 (51.4)	2.5	0.7754
Positive	58	36/58 (62.1)	2.7	
NA*	30			
Vascular invasion				
Negative	53	33/53 (62.3)	3.2	0.1276
Positive	45	25/45 (55.6)	2.5	
NA*	25			

* NA: not available.

Please cite this article in press as: Nagashio R, et al. Expression of RACK1 is a novel biomarker in pulmonary adenocarcinomas. Lung Cancer (2009), doi:10.1016/j.lungcan.2009.09.015